QUANTUM CORRELATIONS IN SPIN CHAINS AND HIGHLY SYMMETRIC STATES

by

Barış Çakmak

Submitted to the Graduate School of Engineering and Natural Sciences
in partial fulfillment of
the requirements for the degree of
Doctor of Philosophy

Sabancı University
Spring 2014

QUANTUM CORRELATIONS IN SPIN CHAINS AND HIGHLY SYMMETRIC STATES

APPROVED BY

Assoc. Prof. Dr. Zafer Gedik .....
(Thesis Supervisor)

Prof. Dr. Cihan Saçlıoğlu .....

Assoc. Prof. Dr. İsmet İnönü Kaya .....

Assoc. Prof. Dr. Özgür Erçetin .....

Prof. Dr. Özgür Esat Müstecaplıoğlu .....

DATE OF APPROVAL .....

QUANTUM CORRELATIONS IN SPIN CHAINS AND HIGHLY SYMMETRIC STATES

Barış Çakmak

Physics, Doctor of Philosophy Thesis, 2014

Thesis Supervisor: Assoc. Prof. Dr. Zafer Gedik

Abstract

Non-classical correlations arise in various quantum mechanical systems. Characterization and quantification of these correlations is an important and active branch of research in the field of quantum information theory. Investigation of non-classical correlations in condensed matter systems gives important insights about the characteristics of these systems. In particular, systems possessing a quantum critical point in their phase diagrams have attracted much attention due to the peculiar behavior of correlations near these points. In this thesis, we have investigated two distinct quantum spin models from the perspective of correlations and, we have discussed the correlation content of an important subclass of bipartite states.

We start by an analytical calculation of the quantum discord for a system composed of spin-j and spin-$1/2$ subsystems possessing rotational symmetry. We have compared our results with the quantum discord of states having similar symmetries and seen that in rotationally invariant states the amount of quantum discord is much higher. Moreover, using the well known entanglement properties of these states, we have compared their quantum discord with entanglement and seen that quantum discord is higher than the entanglement. Next, we have investigated the thermal quantum correlations and entanglement in spin-1 Bose-Hubbard model with two and three particles. We have demonstrated that the energy level crossings in the ground state of the system are signalled by both the behavior of thermal quantum correlations and entanglement. Finally, we have investigated various thermal quantum and total correlations in the anisotropic XY spin-chain with transverse magnetic field. We have shown that the ability of the considered measures to estimate the critical points of this system at finite temperature strongly depends on the anisotropy parameter of the Hamiltonian. Furthermore, we have studied the effect of temperature on long-range correlations of the XY chain.

SPIN ZINCIRLERI VE SIMETRIK HALLERDE KUANTUM ILINTILERI

Barış Çakmak

Fizik, Doktora Tezi, 2014

Tez Danışmanı: Doç. Dr. Zafer Gedik

Özet

Klasik olmayan ilintileri çok çeşitli kuantum mekaniksel sistemdelerde gözlemek mümkündür. Bu ilintilerin karakterizasyonu ve ölçümü, kuantum enformasyon teorisi içerisinde önemli ve halen aktif araştırmanın devam ettiği bir alandır. Çeşitli yoğun madde fiziği sistemlerinde klasik olmayan ilintileri inceleyerek, bu sistemlerle ilgili önemli bilgiler edinilebildiği bilinmektedir. Özellikle faz diyagramında kuantum kritik noktalar bulunduran modellerde ilintilerin kritik nokta etrafındaki beklenmedik davranışı oldukça ilgi çekmiştir. Biz bu çalışmamızda, iki değişik kuantum spin modelini klasik olmayan ilintiler gözüyle inceledik. Ayrıca, iki alt sistemden oluşan kuantum hallerinin önemli bir alt kümesinde, çeşitli ilinti ölçütlerinin nasıl davrandığını tartıştık.

İlk olarak, spin-j ve spin-$1/2$ altsistemlerden oluşan, dönmeler altında değişmez hallerde kuantum uyuşmazlık ölçütünü analitik olarak hesapladık. Sonuçlarımızı benzer simetrilere sahip sistemlerin kuantum uyuşmazlığı ve dolaşıklığı ile karşılaştırdık. İncelediğimiz sistemdeki uyumşmazlık miktarının karşılaştırdığımız hallerdekinden daha fazla olduğunu gözlemledik. İkinci olarak, bir boyutlu XY spin modelinde sonlu sıcaklıkta, çeşitli kuantum ve toplam ilintilerin davranışını araştırdık. Bu ilintilerin kuantum kritik noktayı doğru tespit etmesinin, Hamiltonyen değişkenlerine önemli ölçüde bağlı olduğunu gösterdik. Son olarak, iki ve üç parçacık için spin-1 Bose-Hubbard modelinde sonlu sıcaklıkta dolaşıklık ve daha genel kuantum ilinti ölçütlerinin davranışını inceledik. Sistemdeki taban hal değişikliklerinin iki ölçüt tarafından da işaret edildiğini gösterdik.

Contents

List of Figures

Chapter 1

INTRODUCTION

Multipartite quantum states contain different kinds of correlations which can or cannot be of classical origin. Entanglement has been recognized as the first indicator of non-classical correlations and it lies at the heart of quantum information science [1]. In addition to considered as the main source of quantum computation, cryptography and information processing, it also proved to be very useful in analyzing the behavior of various condensed matter systems [2]. However, entanglement is not the only kind of meaningful correlation present in quantum systems. Quantum discord (QD) [3, 4], defined as the discrepancy between the quantum versions of two classically equivalent expressions for mutual information, is demonstrated to be a novel resource for quantum computation [5–7]. Following the discovery of quantum discord, several new quantifiers of quantum correlations, that are more general than entanglement, have been proposed recently [8-11].

Quantum phase transitions (QPTs) are sudden changes occurring in the ground states of many-body systems when one or more of the physical parameters of the system are continuously varied at absolute zero temperature [8]. These radical changes, which strongly affect the macroscopic properties of the system, are manifestations of quantum fluctuations. Despite the fact that reaching absolute zero temperature is practically impossible, QPTs might still be observed at sufficiently low temperatures, where thermal fluctuations are not significant enough to excite the system from its ground state. In recent years, the methods of quantum information theory have been widely applied to quantum critical systems. Especially, the behavior of non-classical correlations in these systems has been ingestigated.

In this thesis, we focus on two main subjects. First is the analysis of various quantifiers of non-classical correlations in spin chains with a QPT in their phase diagrams. Second, is the analytical calculation of QD in some highly symmetric states.

This thesis is organized as follows. In the second chapter, we provide a simple introduction of the mathematical formalism and tools that will be used throughout the thesis.

In the Chapter 3, we analytically calculate the QD of a rotationally invariant bipartite system. We compare our results with the entanglement properties of rotationally invariant states and other analytical calculations of quantum discord in systems having similar symmetries. We have observed that even though the content of entanglement decreases as j increases, the amount of QD remains significantly larger with its maximum value also following a decreasing trend.

In Chapter 4, we investigate the pairwise thermal quantum and total correlations in one-dimensional anisotropic spin-$1/2$ XY chain with transverse magnetic field. As a measure of genuine quantum correlations, we utilize the entanglement quantified by concurrence [9, 10], and a very recently proposed observable measure (OMQC) [11], which is a simplified version of geometric measure of quantum discord [12]. OMQC has the advantage of not requiring a full tomography of the system, making it very accessible experimentally. On the other hand, in order to quantify non-locality or total correlations in a quantum system, we employ measurement-induced nonlocality (MIN) [13], and an alternative new measure defined in terms of Wigner-Yanase skew information (WYSIM) [14]. By comparatively studying the thermal quantum and total correlations in the parameter space of the Hamiltonian for the first and second nearest neighbor spins, we have observed that all of these measures are capable of indicating the CP of QPT at absolute zero. When the temperature is slightly above absolute zero, i.e. in the experimentally accessible region, we analyze the ability of these correlation measures to accurately estimate the CP of the transition. Finally, we study the long-range correlations of the system and the effect of temperature on these correlations.

In Chapter 5, we analyze the quantum correlations in a spin-1 Bose-Hubbard model with two and three particles by considering periodic boundary conditions. As a measure of quantum correlations, we use a recently introduced measure for an arbitrary bipartite system based on a necessary and sufficient condition for a zero-discord state in the coherence-vector representation of density matrices [15]. On the other hand, we adopt negativity to measure the amount of entanglement in a quantum state. We demonstrate that the quantum correlations that are more general than entanglement and the negativity can mark the critical points corresponding to energy level crossings in the ground state of the system. Although we only consider systems with only few particles in our study, this interesting behavior have the potential to have consequences even for actual quantum critical systems, where the number of particles is very large and the energy level crossings really lead to quantum QPTs.

Chapter 2

BASIC NOTIONS

In the following Chapter, an introduction to elementary concepts in quantum mechanics and quantum information theory will be provided. We begin by introducing how to refer to quantum objects and continue with how to perform measurements on them. Lastly, their evolution in time will be introduced. For additional information on the topics discussed in this chapter, we refer the reader to [16–23].

2.1 Quantum States

Quantum mechanical states are rays in a Hilbert space, $\mathcal{H}$ and they are denoted as $|\psi\rangle$ in so called Dirac notation. A d-dimensional quantum state $|\psi\rangle$, is a d-dimensional complex vector in $\mathcal{H} = \mathcal{C}^d$ which can be written, with its dual $\langle\psi|$, as

$$|\psi\rangle = (c_1, c_2, \cdots, c_d)^T, \langle\psi| = (c_1^*, c_2^*, \cdots, c_d^*)^T, \tag{2.1}$$

with $\langle\psi|\psi\rangle = \sum_i^d |c_i|^2 = 1$, and T the transposition operation. The inner product of two states $|\psi\rangle = (c_1, c_2, \cdots, c_d)^T$ and $|\phi\rangle = (e_1, e_2, \cdots, e_d)^T$ is defined as

$$\langle\psi|\phi\rangle = \sum_i c_i^* e_i. \tag{2.2}$$

We need a set of vectors $\{|x_1\rangle, |x_2\rangle, \cdots, |x_k\rangle\}$, spanning the whole Hilbert space that we are working in such that any state in this Hilbert space can be written as a linear combination of these vectors. This set of vectors is called the basis vectors of the Hilbert space, and they have to be orthogonal to each other, $\langle x_i|x_j\rangle = \delta_{ij}$, where δ_{ij} is the Kronecker-Delta symbol, for all i and j. In terms of these basis vectors, an arbitrary state, say $|\psi\rangle$, can be written as

$$|\psi\rangle = \sum_i c_i |x_i\rangle, \tag{2.3}$$

where $c_i = \langle\psi|x_i\rangle$. Since, in quantum mechanics the interpretation of $|c_i|^2$ is a probability density, c_is have to be normalized to unity, $\sum_i |c_i|^2 = 1$. Another property of the Hilbert space is its linearity which results in one of the most important features of quantum mechanics; superposition. If we are given two states $|\psi\rangle$ and $|\phi\rangle$, a state made up of the linear superposition of these two, is also a valid quantum state and it can be written as

$$|\chi\rangle = a|\psi\rangle + b|\phi\rangle \tag{2.4}$$

with $|a|^2+|b|^2 = 1$. While a relative phase difference between the superposed states, such as $a|\psi\rangle + be^{i\eta}|\phi\rangle$, is physically significant and makes up a different state than the one in Eq. 2.2, an overall phase is physically irrelevant.

For a system composed of more than one quantum state, we need to enlarge the Hilbert space accordingly. Consider two quantum systems $|\psi_A\rangle = (c_{A1}, c_{A2}, \cdots, c_{Ad_A})^T \in \mathcal{H}_\mathcal{A}$ and $|\psi_B\rangle = (c_{B1}, c_{B2}, \cdots, c_{Bd_B})^T \in \mathcal{H}_\mathcal{B}$. Then the composite system of these two particles (a bipartite state) can be represented as a tensor product of them $|\psi_{AB}\rangle = |\psi_A\rangle \otimes |\psi_B\rangle \in \mathcal{H}_\mathcal{A} \otimes \mathcal{H}_\mathcal{B}$. In particular, $|\psi_{AB}\rangle$ can be written as

$$|\psi_{AB}\rangle = (c_{A1}c_{B1}, c_{A1}c_{B2}, \cdots, c_{A1}c_{Bd_B}, c_{A2}c_{B1}, \cdots, c_{Ad_A}c_{Bd_B})^T. \tag{2.5}$$

The generalization of this procedure to multiple states (multipartite state) is straightforward. If we have a set of n states, $\{|\psi_n\rangle\}$ with $n = 1, 2, \cdots$ we can write the collective state of these n states as

$$|\Psi\rangle = |\psi_1\rangle \otimes |\psi_2\rangle \otimes \cdots \otimes |\psi_n\rangle. \tag{2.6}$$

In common quantum information theory notation, such states are written as $|\Psi\rangle = |\psi_1\psi_2\cdots\psi_n\rangle$, omitting the tensor product symbol.

2.2 The Density Matrix

We have introduced the state space of quantum states. However, in some cases, it is not possible to have an exact knowledge about the system and talk about a single state vector. Instead, the system might be composed of a mixture of multiple state vectors. In order to extend our formalism to also cover these kind of quantum states, we now introduce the density matrix formalism.

Consider a quantum system which is in one of the states $|\psi_i\rangle$ with probability p_i. These quantum states along with their probabilities form an ensemble, $\{p_i, \psi_i\rangle\}$. In this

case, we can write the density matrix of the system in the following way

$$\rho = \sum_i p_i |\psi_i\rangle\langle\psi_i|, \tag{2.7}$$

where, due to the normalization of probabilities, $\sum_i p_i = 1$. Quantum systems for which the state vector is known we can write the density matrix as $\rho = |\psi\rangle\langle\psi|$. These states are called as pure quantum states. On the other hand, if the considered system is a mixture of state vectors from an ensemble of pure states, $\{p_i, \psi_i\rangle\}$, it is called a mixed state. Here, mixing is completely classical and should not be confused with the purely quantum feature of superposition.

We now list the general properties that must be satisfied to be a valid density matrix:

- ρ is an Hermitian matrix

$$\rho = \sum_i p_i |\psi_i\rangle\langle\psi_i| = \rho^\dagger. \tag{2.8}$$

- ρ is a positive operator

$$\begin{aligned} \langle\chi|\rho|\chi\rangle = \ & \textstyle\sum_i p_i \langle\chi|\psi_i\rangle\langle\psi_i|\chi\rangle, \\ & \textstyle\sum_i p_i |\langle\chi|\psi_i\rangle|^2 \geq 0. \end{aligned} \tag{2.9}$$

- The sum of the diagonal elements of ρ must add up to unity

$$\mathrm{Tr}(\rho) = 1. \tag{2.10}$$

A natural consequence of the above properties is that the inequality $\mathrm{Tr}(\rho^2) \leq 1$ holds for all ρ with inequality saturated only for pure states for which $\rho^2 = |\psi_i\rangle\langle\psi_i|\psi_i\rangle\langle\psi_i| = |\psi_i\rangle\langle\psi_i| = \rho$. This inequality gives us an easy way to determine if a given quantum state is pure or mixed.

Similar to the case of state vectors, the density matrix of a bipartite state is written as the tensor product of its subsystems

$$\rho_{AB} = \rho_A \otimes \rho_B. \tag{2.11}$$

It is important to note that not all composite bipartite density matrices admit such a nice decomposition in terms of the density matrices of their subsystems. Such states are called entangled, and they will be further discussed in the subsequent chapter.

2.2.1 The Reduced Density Matrix

The density matrix can also be used as a tool to describe its subsystems. The way to do this is to obtain the reduced density matrix of the composite system, which corresponds to the density matrix for one of the subsystems. For example for a bipartite system ρ_{AB}. Then, the reduced density matrix for ρ_A is

$$\rho_A = \text{Tr}_B(\rho_{AB}), \tag{2.12}$$

where Tr_B is the the partial trace operation. We can perform this operation as follows

$$\begin{aligned} \text{Tr}_B(|a_1\rangle\langle a_2| \otimes |b_1\rangle\langle b_2|) &= \sum_i \langle e_i|(|a_1\rangle\langle a_2| \otimes |b_1\rangle\langle b_2|)|e_i\rangle \\ &= \sum_i |a_1\rangle\langle a_2|\langle e_i|b_1\rangle\langle b_2|e_i\rangle \\ &= |a_1\rangle\langle a_2|\langle \text{Tr}(|b_1\rangle\langle b_2|) \\ &= |a_1\rangle\langle a_2|\langle y_1|y_2\rangle, \end{aligned} \tag{2.13}$$

where the set $\{e_i\}$ denoted an orthonormal basis in $\mathcal{H}_\mathcal{B}$. As demonstrated above, the partial trace operation is the same as the usual trace operation except that it is performed only on the subsystem that we want to leave out.

2.3 Measurement

All physical theories have physical observables which can be measured by an observer. In quantum mechanics, the observables, A, are Hermitian (self-adjoint) operators, $A = A^\dagger$. The measurements of these observables are described by a set of operators $\{M_m\}$, where m labels the possible outcomes of the measurement. These operators act on the Hilbert space of the measured system. The probability of getting the result m after a measurement on a given state $|\psi\rangle$ is given as

$$p_m = \langle\psi|M_m^\dagger M_m|\psi\rangle, \tag{2.14}$$

with the post-measurement state in the following form

$$\frac{M_m|\psi\rangle}{\sqrt{\langle\psi|M_m^\dagger M_m|\psi\rangle}}. \tag{2.15}$$

The set of measurement operators have to satisfy the completeness relation $\sum_m M_m^\dagger M_m = 1$, due to the fact that the probabilities measurement outcomes must add up to unity. Main principles behind the measurement of a quantum system gives us two important items of information about the system. First one is the probability of getting a specific outcome and the post-measurement state.

The measurement theory introduced for state vectors can easily be generalized to density matrix formalism. In this case, the probability of getting the outcome m after a measurement is calculated as $p_m = \text{Tr}(M_m^\dagger M_m \rho)$ and the post measurement state can be written as

$$\frac{M\rho M^\dagger}{\text{Tr}(M_m^\dagger M_m \rho)}. \tag{2.16}$$

In many applications of quantum theory when we are talking about a measurement, we are talking about a projective measurement which is a special case of the general measurements introduced above. After such a measurement, the measured state is projected on the measured eigenstate of the observable. Therefore, if a second measurement is made just after the first one, the outcome will be the same. Therefore, one can repeatedly perform the projective measurements on a given system. On top of the conditions that are listed above, a set of projective measurement operators have to satisfy $P_m P_{m'} = \delta_{mm'} P_m$, i.e. they must be orthogonal to each other.

On the other hand, in real physical scenarios, sometimes we may not know the post measurement state, but we may want to learn the possible measurement outcomes. In such cases the Positive Operator-Valued Measure (POVM) formalism is a very powerful tool to analyze such cases. There two widespread jargon to refer such measurements. They are either called POVM measurements or non-orthogonal measurements. We have seen that the probability of getting the outcome m after the measurement M_m is performed is $p_m = \langle\psi|M_m^\dagger M_m|\psi\rangle$. Suppose now, we define

$$E_m = M_m^\dagger M_m. \tag{2.17}$$

The set of operators $\{E_m\}$ satisfies all the criteria to be a measurement operator, and they are sufficient to determine the probability of a measurement outcome. The set $\{E_m\}$ is called POVM and a single operator E_m in this set is called a POVM element. POVM measurements are non-repeatable, contrary to the case of projective measurements, since the post-measurement state of the system is unknown. Also they do not have the restriction to be orthogonal to each other, hence the name non-projective measurements.

POVM measurements provide a more general approach to the measurement of a quan-

tum system compared to the projective measurements. However, it is important to note that, projective measurements in an enlarged Hilbert space is completely equivalent to POVM measurements in the Hilbert space before the enlargement [x]. This result is called the Neumark's Theorem [x].

2.4 Dynamics

In this section we will introduce how closed quantum states evolves in time. The word closed here refers to to an isolated system where no interactions with the surrounding environment is allowed. For such a system, the evolution is described by a unitary transformation

$$|\psi(t_2)\rangle = U(t_2, t_1)|\psi(t_1)\rangle, \tag{2.18}$$

where U satisfies the relation $U^{-1} = U^\dagger$ with $U^\dagger$ being the Hermitian conjugate (conjugate-transpose) of U. Necessity for a unitary operator rises from the fact that any transformation made on a quantum state has to conserve the length of the state vectors. However, up to this point we do not have any information about which unitary transformations correspond to the dynamics realized in a quantum system. To have such a knowledge, we need to know how a particular quantum state $|\psi\rangle$ changes in time. Answer to this question is given by the Schrödinger equation

$$i\hbar\frac{d}{dt}|\psi\rangle = H|\psi\rangle \tag{2.19}$$

where H is the Hamiltonian of the system which is an Hermitian matrix and $\hbar$ is the Planck's constant. In fact, the operator $U(t_2, t_1)$, which characterizes the transformation of the quantum state from time t_1 to t_2, can be deterministically found by solving the Scrödinger equation. As a special case, for a time-independent Hamiltonian, it is possible write $U(t_2, t_1)$ in a compact form

$$|\psi(t_2)\rangle = \exp\left[\frac{-iH(t_2 - t_1)}{\hbar}\right] = U(t_2, t_1)|\psi(t_1)\rangle. \tag{2.20}$$

Here $U(t_2, t_1) = \exp[(-iH(t_2 - t_1))/\hbar]$ is defined as the time evolution operator, also known as the propagator.

Time evolution of the density matrices isolated from the environment can also be formulated in the same framework. An arbitrary density matrix at an arbitrary time t_2 can

be written as

$$\rho(t_2) = \sum_i p_i |\psi_i(t_2)\rangle\langle\psi_i(t_2). \tag{2.21}$$

Then, following from (2.18)

$$\begin{aligned} \rho(t_2) \quad &= \sum_i p_i U(t_2,t_1)|\psi_i(t_1)\rangle\langle\psi_i(t_1)U^\dagger(t_2,t_1) \\ &= U(t_2,t_1)\rho(t_1)U^\dagger(t_2,t_1). \end{aligned} \tag{2.22}$$

Scrödinger equation can be employed to determine the equation of motion for density matrices

$$\begin{aligned} \frac{d}{dt}\rho(t) \quad &= \sum_i p_i \left(\frac{d}{dt}|\psi_i(t)\rangle\right)\langle\psi_i(t)| + |\psi_i(t)\rangle\left(\frac{d}{dt}\langle\psi_i(t)|\right) \\ &= \frac{1}{i\hbar}(H\rho(t) - \rho(t)H) = \frac{1}{i\hbar}[H,\rho(t)]. \end{aligned} \tag{2.23}$$

Above equation is known as the von-Neumann equation.

2.5 Spin of a Particle

Spin is a fundamental property of all elementary quantum objects, such as mass or charge. It interacts with external magnetic fields or with the spin of an other particle, just like the charged particles interact with external electric fields or other charged particles. It is a vector quantity; it has both a direction in the space and a magnitude. Magnitude of the spin is quantized on a given direction. Allowed values of the magnitude of the spin is determined by the spin quantum number s which can take the values $s = n/2$ with n being a non-negative integer. The spin quantum number depends only on the type of the quantum particle. Mathematically, we can express the spin $\mathbf{S}$ as follows

$$\mathbf{S} = \mathbf{S}_x + \mathbf{S}_y + \mathbf{S}_z, \tag{2.24}$$

where $\mathbf{S}_x$, $\mathbf{S}_y$ and $\mathbf{S}_z$ denotes the components of the vector $\mathbf{S}$. These components obey the following relation

$$[S_i, S_j] = i\hbar\epsilon_{ijk}S_k. \tag{2.25}$$

Here, $i,j,k \in \{x,y,z\}$, $[A,B] = AB - BA$ denotes the commutator and ϵ_{ijk} is the antisymmetric Levi-Civita symbol. Before proceeding to special cases, it is very important

to note that, although the name suggests a picture of rotation of a particle around its own axis, this is wrong. Spin has no classical counterpart.

2.5.1 Spin-$1/2$

The special case of $s = 1/2$ is important because the well-known elementary particles, such as electron, proton and neutron, fall into this case. Moreover, central to quantum information theory, the quantum bit, widely known as qubit, can be represented by a spin-$1/2$ particle. For a spin-$1/2$ particles components of the spin operator are denoted by σ and have the following explicit matrix forms

$$\sigma_x = \begin{pmatrix} 0 & 1 \\ 1 & 0 \end{pmatrix}, \qquad \sigma_y = \begin{pmatrix} 0 & -i \\ i & 0 \end{pmatrix}, \qquad \sigma_z = \begin{pmatrix} 1 & 0 \\ 0 & -1 \end{pmatrix}. \tag{2.26}$$

These matrices are also called Pauli matrices and together with the identity matrix, any 2×2 Hermitian matrix can be written as a linear combination of them. In a given direction in space, spin-$1/2$ particles can either be parallel to that direction or antiparallel to it, with its magnitude equal to $\hbar/2$ or $-\hbar/2$, respectively.

Connection with the qubit comes at this point. A classical bit can only have two values, 0 or 1. However, in quantum mechanics we can have a superposition of these two states

$$|\psi\rangle = a|0\rangle + |1\rangle, \tag{2.27}$$

where $|a|^2 + |b|^2 = 1$. Since spin-$1/2$ particles can be in two different states, as mentioned earlier, they provide a natural physical setting for qubits. Generalization to higher dimensional states, for example a three level system (qutrit), is again possible by considering particles with higher spin quantum numbers.

Chapter 3

QUANTUM CORRELATIONS

In this chapter we will review the main concepts and measures of quantum correlations. We will start our discussion by introducing the concept of entanglement and continue with its quantifiers. Next, we will turn our attention to the quantum correlations that are more general than entanglement. Our main focus in this part will be on the notion of quantum discord. We will finish this chapter by introducing quantifiers of total correlations.

3.1 Entanglement

Entanglement has been recognized as the first indicator of non-classical correlations and lies at the heart of quantum information science [21–23]. Its properties and behavior in various different settings have been vastly investigated in the literature [1]. In the following chapters, we will consider the behavior of different entanglement quantifiers in two different spin chain models. We start by defining the states which are not entangled. These states are called separable states and they have a unique form. Consider a pure bipartite state, $|\psi_{AB}\rangle$, living in the Hilbert space $\mathcal{H}_{\mathcal{A}} \otimes \mathcal{H}_{\mathcal{B}}$. $|\psi_{AB}\rangle$ is separable if and only if it can be written in the form

$$|\psi_{AB}\rangle = |\psi_A\rangle \otimes |\psi_B\rangle. \tag{3.1}$$

Here, $|\psi_A\rangle \in \mathcal{H}_{\mathcal{A}}$ and $|\psi_B\rangle \in \mathcal{H}_{\mathcal{B}}$ are the two subsystems of $|\psi_{AB}$. In other words, if a composite system can be written as a direct product of its constituents, it is separable. Next, we turn our attention to mixed bipartite states. We have explained that for mixed states, it is not possible to characterize the system with a single state vector. In this case, if the density matrix the total system, ρ_{AB}, admits a decomposition of the form

$$\rho_{AB} = \sum_i p_i \rho_A \otimes \rho_B, \tag{3.2}$$

with $\sum_i p_i$, it is said to be separable, otherwise it is entangled [24]. Although criterion for separability is straightforward to check for pure states, the task of determining if an arbitrary mixed state is separable or not in not easy in general. We will now introduce a general strict criterion for separability.

3.2 Peres-Horodecki Criterion for Separability

There is a necessary condition for separability of bipartite states introduced by Peres, based on the partial transposition operation [25]. Lets say we have the following density matrix

$$\rho_{AB} = \sum_{ijkl} p_{ij}^{kl} |i\rangle\langle j| \otimes |k\rangle\langle l|. \tag{3.3}$$

Taking the partial transpose of this matrix with respect to the subsystem B, yields the following result

$$\rho_{AB}^{T_B} = \sum_{ijkl} p_{ij}^{kl} |i\rangle\langle j| \otimes |l\rangle\langle k|. \tag{3.4}$$

Separability criterion states that if ρ_{AB} is separable, then $\rho_{AB}^{T_B}$ has non-negative eigenvalues. It is also known as the positive partial transpose (PPT) criterion. It is important to note that this criterion is only necessary and not sufficient in general. However, if the Hilbert space dimensions of the subsystems are both 2 (two spin-$1/2$ particles) or one of them is 2 while the other is 3 (a spin-$1/2$ and a spin-1 particles), the criterion is both necessary and sufficient [26].

3.3 Entanglement Measures

Now that we know how to determine the separable states, we will now move on to the subject of how to quantify the entanglement contained in an entangled state. This is a vastly explored subject, since entanglement is central to almost all applications in quantum information theory [1]. But first, we need to introduce the concept of local operations and classical communication (LOCC) [27–30]. In LOCC setting, distant parties that are sharing a quantum system can only apply local operations to their subsystems and they can only classically communicate with each other, transmitting quantum information is forbidden. The natural necessity for this protocol arises from the fact that classical communication cannot increase entanglement and as a result it is kept as a resource to be manipulated. For an arbitrary bipartite density matrix, LOCC operations can be written

in the form

$$\Gamma(\rho) = \sum_i A_i \otimes B_i \rho A_i^\dagger \otimes B_i^\dagger, \tag{3.5}$$

where A_i and B_i are the generalized measurement operators acting on the Hilbert space of subsystems A and B, respectively.

There is a list of reasonable assumptions in order fully characterize the entanglement content of a given state. Any good measure of entanglement, say E, is a mapping that takes density matrices as input and produces positive real numbers as output. Such a mapping is expected to satisfy the following features

- $E(\rho)$ vanishes if ρ is a separable state.
- Entanglement is invariant under local unitary transformations, $E(\rho) = U_A \otimes U_B \rho U_A^\dagger \otimes U_B^\dagger$
- The mapping E is an entanglement monotone, meaning it does not increase under LOCC operations on average

  $$E(\rho) \geq \sum_i p_i E(\rho_i), \tag{3.6}$$

  where p_i denotes the probability of obtaining ρ_i after the LOCC.

There are some other properties such as normalization, convexity etc., which may be useful in some context. But the above requirements are the only ones that is necessary for an entanglement measure [31–36]. We will now move on to introduce some entanglement measures, that will be utilized in the following chapters.

3.3.1 Entropy of Entanglement

In order to define entropy of entanglement, we first define the von-Neumann entropy, which is the generalization of Shannon entropy in classical information theory to the quantum systems. Shannon entropy [37], gives us the amount of information that we get after measuring a random variable X with possible values $\{x_1, x_2, \cdots, x_n\}$. Explicitly, it is given by the expression

$$H(p(x_1), p(x_2), \cdots, p(x_n)) = -\sum_i p(x_i) \log p(x_i), \tag{3.7}$$

where the log denoted the logarithm to the base 2. By replacing the probability distribution with density matrix, quantum version of Shannon entropy, von-Neumann entropy is

defined as

$$S(\rho) = -\sum_i \lambda_i \log \lambda_i, \tag{3.8}$$

where λ_i are the eigenvalues of the density matrix.

Having defined the von-Neumann entropy, we now have the necessary tools to define the entropy of entanglement [38]. For a pure bipartite density matrix, ρ_{AB}, the entropy of entanglement is given by

$$E_E(\rho_{AB}) = S(\rho_A) = S(\rho_B). \tag{3.9}$$

Here, $\rho_A = \mathrm{Tr}_B(\rho_{AB})$ and $\rho_B = \mathrm{Tr}_A(\rho_{AB})$ are the reduced density matrices for the subsystems A and B, respectively. The fact that the composite system is a pure state, does not guarantee that its reduced density operators will also be pure. In fact, a maximally mixed reduced density matrix, $\rho_A = \rho_B = I/2$ where I is the identity matrix in the appropriate Hilbert space dimension, implies that the pure composite system is maximally entangled, hence the entropy entanglement is maximum. This maximum scales with the logarithm of the Hilbert space dimension, $\log d$.

3.3.2 Concurrence

Concurrence is a well-defined and remarkably easy entanglement measure for two spin-$1/2$ density matrices [9, 10]. In order to evaluate concurrence, one first needs to calculate the time-reversed or spin-flipped density matrix $\tilde{\rho}$ which is given by

$$\tilde{\rho} = (\sigma^y \otimes \sigma^y)\rho^*(\sigma^y \otimes \sigma^y). \tag{3.10}$$

Here σ^y is the Pauli spin operator and ρ^* is obtained from ρ via complex conjugation. Then, concurrence reads

$$C(\rho) = \max\left\{0, \sqrt{\lambda_1} - \sqrt{\lambda_2} - \sqrt{\lambda_3} - \sqrt{\lambda_4}, \right\}, \tag{3.11}$$

where $\{\lambda_i\}$ are the eigenvalues of the product matrix $\rho\tilde{\rho}$ in decreasing order.

In the special case of X-shaped density matrix

$$\rho^{ab} = \begin{pmatrix} \rho_{11} & 0 & 0 & \rho_{14} \\ 0 & \rho_{22} & \rho_{23} & 0 \\ 0 & \rho_{23} & \rho_{22} & 0 \\ \rho_{14} & 0 & 0 & \rho_{44} \end{pmatrix}, \tag{3.12}$$

which we will encounter in the following chapters, concurrence reduces to

$$C = 2\max\{0, |\rho_{14}| - |\rho_{22}|, |\rho_{23}| - \sqrt{\rho_{11}\rho_{44}}\}. \tag{3.13}$$

3.3.3 Entanglement of Formation

A resource based measure of entanglement for an arbitrary bipartite state (including mixed states) is given by the entanglement of formation [10]. It is defined as follows

$$E_F(\rho_{AB}) = \min p_i E(|\psi_i\rangle). \tag{3.14}$$

Here, the minimization is made over all possible sets of pure states $\mathcal{E} = \{p_i, |\psi\rangle\}$ that yields the given state $\rho_{AB} = \sum_i p_i |\psi_i\rangle\langle\psi_i|$ and $E(.)$ is the entropy entanglement. Actually, EoF is nothing but an extension of entropy of entanglement to mixed states. Naturally, it converges to E_E for pure states. The reason that EoF is a resource based measure is that it quantifies the number of maximally entangled states to construct the given state. Therefore, it is of operational importance. For pure two spin-$1/2$ density matrices, EoF can be expressed in terms of the concurrence

$$EoF(\rho) = h\left(\frac{1+\sqrt{1-C^2(\rho)}}{2}\right), \tag{3.15}$$

where $h(x) = -x\log(x) - (1-x)\log(1-x)$. However, in most cases it is not possible to find an analytic formula for EoF due to the optimization procedure.

3.3.4 Negativity

Negativity is a measure of entanglement that can be straightforwardly calculated for an arbitrary bipartite system in all Hilbert space dimensions. Although we cannot conclude whether a PPT state (zero negativity state) is entangled or separable in general, negativity is still a reliable measure for all negative partial transpose states [39]. For a given bipartite density matrix ρ_{AB}, it can be defined as the absolute sum of the negative eigenvalues of partial transpose of ρ_{AB} with respect to the smaller dimensional system,

$$N(\rho_{AB}) = \frac{1}{2}\sum_i |\eta_i| - \eta_i, \tag{3.16}$$

where η_i are all of the eigenvalues of the partially transposed density matrix $(\rho_{AB})^{T_B}$.

3.4 Quantum Discord

Recent research on quantum correlations has shown that entanglement is not the only kind of useful quantum correlation. Quantum discord (QD), which is defined as the discrepancy between two classically equal descriptions of quantum mutual information, has also proven to be utilizable in quantum computing protocols [3–5]. Moreover, QD is more general than entanglement in the sense that it can be present in separable mixed quantum states as well. Following this discovery, much effort has been put into investigating the properties and behavior of QD in various systems ranging from quantum spin chains to open quantum systems [7]. Nevertheless, since evaluation of QD requires a very complex optimization procedure, the significant part of the development in the field is numeric and analytical results are present only for some very restricted set of states. In general, these restrictions are introduced by forcing certain symmetries and limiting the size and the dimension of the system under consideration. A short list of analytical results would include the progress in, X-shaped states of different dimensions [40–44], $2\otimes d$ dimensional two-parameter class of states [45], $d\otimes d$ dimensional Werner and pseudo-pure states [46], general real density matrices displaying Z_2 symmetry [47], two-mode Gaussian states [48], and $2 \otimes d$ dimensional mixed states of rank-2 [49–51] where d denotes the Hilbert space dimension of the system under consideration. QD witnesses have also been introduced for $2 \otimes d$ systems [52]. Following QD, many other quantum and total correlation quantifiers have been introduced [12–14, 53–55].

We will now review the concept of quantum discord. We have very briefly mentioned that quantum discord is the difference between the quantum extensions of the classical mutual information. First and direct generalization of classical mutual information is obtained by replacing the Shannon entropy with its quantum analog, the von Neumann entropy

$$I(\rho^{ab}) = S(\rho^a) + S(\rho^b) - S(\rho^{ab}). \tag{3.17}$$

Here, ρ^a and ρ^b are the reduced density matrices of the subsystems and $S(\rho) = -\text{tr}\rho\log_2\rho$ is the von Neumann entropy. On the other hand, in classical information theory, mutual information can also be written in terms of the conditional probability. However, generalization of conditional probability to quantum case is not straightforward since the uncertainty in a measurement performed by one party depends on the choice of measurement. Therefore, one has to optimize over the set of measurements made on a system

[3, 4]

$$C(\rho^{ab}) = S(\rho^a) - \min_{\{\Pi_k^b\}} \sum_k p_k S(\rho_k^a), \tag{3.18}$$

where, in this work, $\{\Pi_k^b\}$ is always understood to be the complete set of one-dimensional projective measurements performed on subsystem b and $\rho_k^a = (I \otimes \Pi_k^b)\rho^{ab}(I \otimes \Pi_k^b)/p_k$ are the post-measurement states of subsystem a after obtaining the outcome k with probability $p_k = \text{tr}(I^a \otimes \Pi_k^b \rho^{ab})$ from the measurements made on subsystem b. $C(\rho)$ can physically be interpreted as the maximum information gained about the subsystem a after the measurements on subsystem b while creating the least disturbance on the overall quantum system. This quantity is also referred as classical correlations contained in a state [4, 7]. Since classical versions of the aforementioned expressions for quantum mutual information are the same, one can define a measure for quantum correlations, namely the quantum discord as

$$D(\rho^{ab}) = I(\rho^{ab}) - C(\rho^{ab}). \tag{3.19}$$

Main challenge in the calculation of quantum discord is the evaluation of classical correlations, since it requires a complex optimization over all measurements on the system. The reason that there is no general analytical results on quantum discord except for very few special cases, is due to this difficulty. It is important to note that quantum discord is dependent on which subsystem the measurements are done. Since making the measurements on spin-j subsystem will make the optimization procedure even harder, in this work, all measurements are made on the spin-$1/2$ subsystem. Furthermore, QD can increase or decrease under local operations and classical communication (LOCC) if the LOCC is performed on the measured part of the system [56–59]. This is a rather peculiar behavior since invariance under LOCC is the defining property of entanglement.

3.4.1 Geometric quantum discord

Geoetric measure of quantum discord (GMQD) has been introduced to overcome the difficulties in the evaluation of the original QD [12]. It measures the nearest distance between a given state and the set of zero-discord states. Mathematically, it is given by

$$D_G(\rho^{ab}) = 2 \min_{\chi} \|\rho^{ab} - \chi\|^2, \tag{3.20}$$

where the minimum is taken over the set of zero-discord states. In a recent work, Girolami et al. have obtained an interesting analytical formula for the GMQD of an arbitrary two-

qubit state [11]

$$D_G(\rho^{ab}) = 2(\mathrm{tr}S - \max\{k_i\}), \tag{3.21}$$

where $S = \vec{x}\vec{x}^t + TT^t$ and

$$k_i = \frac{\mathrm{tr}S}{3} + \frac{\sqrt{6\mathrm{tr}S^2 - 2(\mathrm{tr}S)^2}}{3}\cos\left(\frac{\theta + \alpha_i}{3}\right), \tag{3.22}$$

with $\{\alpha_i\} = \{0, 2\pi, 4\pi\}$ and $\theta = \arccos\{(2\mathrm{tr}S^3 - 9\mathrm{tr}S\mathrm{tr}S^2 + 9\mathrm{tr}S^3)\sqrt{2/(3\mathrm{tr}S^2 - (\mathrm{tr}S)^2)^3}\}$. Furthermore, observing that $\cos\left(\frac{\theta+\alpha_i}{3}\right)$ reaches its maximum for $\alpha_i = 0$ and choosing θ to be zero, they have found a very tight lower bound to the GMQD, given by

$$Q(\rho^{ab}) = \frac{2}{3}(2\mathrm{tr}S - \sqrt{6\mathrm{tr}S^2 - 2(\mathrm{tr}S)^2}). \tag{3.23}$$

This quantity, that we will refer as observable measure of quantum correlations (OMQC), can be regarded as a meaningful measure of quantum correlations on its own and it has the desirable feature that it needs no optimization procedure. Besides being easier to manage than the original GMQD, it can be measured by performing seven local projections on up to four copies of the state. Thus, $Q(\rho)$ is also very experimentally friendly since one does not need to perform a full tomography of the state.

3.5 Non-classical Correlation Measures

In this section, we briefly review the remaining non-classical correlation measures used in our this thesis.

3.5.1 Coherence-vector based measure

We first introduce a measure of non-classical correlations proposed by Zhou et al. based on a necessary and sufficient condition for a zero-discord state [15]. A general bipartite state ρ^{ab} can be expressed in coherence-vector representation as

$$\begin{aligned}\rho^{ab} \quad &= \tfrac{1}{mn} I^a \otimes I^b + \textstyle\sum_{i=1}^{m^2-1} x_i X_i \otimes \frac{I^b}{2n} + \frac{I^a}{2m} \otimes \sum_{j=1}^{n^2-1} y_j Y_j \\ &\quad + \tfrac{1}{4}\textstyle\sum_{i=1}^{m^2-1}\sum_{j=1}^{n^2-1} t_{ij} X_i \otimes Y_j,\end{aligned} \tag{3.24}$$

where the matrices $\{X_i : i = 0, 1, \cdots, m^2-1\}$ and $\{Y_j : j = 0, 1, \cdots, n^2-1\}$, satisfying $\mathrm{tr}(X_k X_l) = \mathrm{tr}(Y_k Y_l) = 2\delta_{kl}$, define an orthonormal Hermitian operator basis associated to the subsystems a and b, respectively. Here, I is the identity matrix for the specified subsystem. The components of the local Bloch vectors $\vec{x} = \{x_i\}$, $\vec{y} = \{y_j\}$ and the

correlation matrix $T = t_{ij}$ can be obtained as

$$\begin{aligned} x_i &= \text{tr}\rho^{ab}(X_i \otimes I^b), \\ y_j &= \text{tr}\rho^{ab}(I^a \otimes Y_j), \\ t_{ij} &= \text{tr}\rho^{ab}(X_i \otimes Y_j). \end{aligned} \tag{3.25}$$

By making use of the above representation of bipartite quantum states, the measure of non-classical correlations is given by

$$\mathcal{Q}(\rho^{ab}) = \frac{1}{4}\sum_{i=m}^{m^2-1} |\Lambda_i|, \tag{3.26}$$

where Λ_i are the eigenvalues of the criterion matrix $\Lambda = TT^t - \vec{y}^t\vec{y}\vec{x}\vec{x}^t$ in decreasing order. The motivation behind the definition of this measure and details of its derivation can be found in Ref. [6].

3.5.2 Measurement-induced non-locality

We will commence by introducing measurement-induced non-locality (MIN) which encapsulates more general kind of correlations than quantum non-locality connected with the violation of Bell inequalities [13]. It is defined by (taking into account the normalization)

$$N(\rho^{ab}) = 2\max_{\Pi^a} \|\rho^{ab} - \Pi^a(\rho^{ab})\|^2, \tag{3.27}$$

where the maximum is taken over the von Neumann measurements $\Pi^a = \{\Pi^a_k\}$ that do not change ρ^a locally, meaning $\sum_k \Pi^a_k \rho^a \Pi^a_k = \rho^a$, and $\|.\|^2$ denotes the square of the Hilbert-Schmidt norm. MIN aims to capture the non-local effect of the measurements on the state ρ^{ab} by requiring that the measurements do not disturb the local state ρ^a. It is always possible to represent a general bipartite state in Bloch basis as

$$\begin{aligned} \rho^{ab} = \frac{1}{\sqrt{mn}}\frac{I^a}{\sqrt{m}} \otimes \frac{I^b}{\sqrt{n}} + \sum_{i=1}^{m^2-1} x_i X_i \otimes \frac{I^b}{\sqrt{n}} \\ + \frac{I^a}{\sqrt{m}} \otimes \sum_{j=1}^{n^2-1} y_j Y_j + \sum_{i=1}^{m^2-1}\sum_{j=1}^{n^2-1} t_{ij} X_i \otimes Y_j, \end{aligned} \tag{3.28}$$

where the matrices $\{X_i : i = 0, 1, \cdots, m^2 - 1\}$ and $\{Y_j : j = 0, 1, \cdots, n^2 - 1\}$, satisfying $\text{tr}(X_k X_l) = \text{tr}(Y_k Y_l) = \delta_{kl}$, define an orthonormal Hermitian operator basis associated to the subsystems a and b, respectively. The components of the local Bloch

vectors $\vec{x} = \{x_i\}$, $\vec{y} = \{y_j\}$ and the correlation matrix $T = t_{ij}$ can be obtained as

$$\begin{aligned} x_i &= \text{tr}\rho^{ab}(X_i \otimes I^b)/\sqrt{n}, \\ y_j &= \text{tr}\rho^{ab}(I^a \otimes Y_j)/\sqrt{m}, \\ t_{ij} &= \text{tr}\rho^{ab}(X_i \otimes Y_j). \end{aligned} \tag{3.29}$$

Although a closed formula for the most general case of bipartite quantum systems is not known, provided that we have a two-qubit system ($m = n = 2$), MIN can be analytically evaluated as

$$N(\rho) = \begin{cases} 2(\text{tr}TT^t - \frac{1}{\|\vec{x}\|^2}\vec{x}^t TT^t\vec{x}) & \text{if } \vec{x} \neq 0, \\ 2(\text{tr}TT^t - \lambda_3) & \text{if } \vec{x} = 0, \end{cases} \tag{3.30}$$

where TT^t is a 3×3 dimensional matrix with λ_3 being its minimum eigenvalue, and $\|\vec{x}\|^2 = \sum_i x_i^2$ with $\vec{x} = (x_1, x_2, x_3)^t$. Due to the symmetries of the considered system in this work, the two-spin reduced density matrix is X-shaped

$$\rho^{ab} = \begin{pmatrix} \rho_{11} & 0 & 0 & \rho_{14} \\ 0 & \rho_{22} & \rho_{23} & 0 \\ 0 & \rho_{23} & \rho_{22} & 0 \\ \rho_{14} & 0 & 0 & \rho_{44} \end{pmatrix}. \tag{3.31}$$

Since the local Bloch vector $\vec{x}$ is never zero in our investigation, MIN takes the simple form

$$N(\rho) = 4(\rho_{23}^2 + \rho_{14}^2). \tag{3.32}$$

3.5.3 Wigner-Yanase information based measure

A new measure of total correlations has been proposed in Ref. [14] by making use of the notion of Wigner-Yanase skew information

$$I(\rho, X) = -\frac{1}{2}\text{tr}[\sqrt{\rho}, X]^2, \tag{3.33}$$

which has been first introduced by Wigner and Yanase [60]. Here X is an observable (an Hermitian operator) and $[.,.]$ denotes commutator. For pure states, $I(\rho, X)$ reduces to the variance $V(\rho, X) = \text{tr}\rho X^2 - (\text{tr}\rho X)^2$. Since the skew information $I(\rho, X)$ depends both on the state ρ and the observable X, Luo introduced an average quantity in order to get

an intrinsic expression

$$Q(\rho) = \sum_i I(\rho, X_i), \tag{3.34}$$

where $\{X_i\}$ is a family of observables which constitutes an orthonormal basis. Global information content of a bipartite quantum system ρ^{ab} with respect to the local observables of the subsystem a can be defined by

$$Q_a(\rho^{ab}) = \sum_i I(\rho^{ab}, X_i \otimes I^b), \tag{3.35}$$

which does not depend on the choice of the orthonormal basis $\{X_i\}$. Then, the difference between the information content of ρ^{ab} and $\rho^a \otimes \rho^b$ with respect to the local observables of the subsystem a can be adopted as a correlation measure for ρ^{ab},

$$\begin{aligned} F(\rho^{ab}) &= \frac{2}{3}(Q_a(\rho^{ab}) - Q_a(\rho^a \otimes \rho^b)), \\ &= \frac{2}{3}(Q_a(\rho^{ab}) - Q_a(\rho^a)), \end{aligned} \tag{3.36}$$

where we add a normalization factor $2/3$. Despite the fact that the evaluation of most of the measures requires a potentially complex optimization process, $F(\rho^{ab})$ (referred as WYSIM) has the advantage that it can be calculated straightforwardly. At this point, we note that quantum mutual information (QMI) has been widely used as the original measure of total correlations contained in quantum states. Being based on the von Neumann entropy, QMI is a well established measure from the communication perspective, while WYSIM is based on the skew information and has a fundamental role in quantum estimation theory [14].

Chapter 4

QUANTUM DISCORD OF $SU(2)$ INVARIANT STATES

4.1 Definition and Entanglement Properties of $SU(2)$ Invariant States

Bipartite $SU(2)$ invariant states are defined by their invariance under rotation of both spins, $U_1 \otimes U_2 \rho U_1^\dagger \otimes U_2^\dagger = \rho$, where $U_{1(2)} = \exp(i\vec{\alpha} \cdot \vec{S}_{1(2)})$ is the usual rotation operator and the length of $\vec{\alpha}$ is chosen according to the spin length $|\vec{S}|$ [61, 62]. In other words, these states commute with every component of the total spin operator $\vec{J} = \vec{S}_1 + \vec{S}_2$. Explicitly, in the total spin basis, for a spin-j_1 and spin-j_2 system, the density matrix of $SU(2)$ invariant states can be written as

$$\rho = \sum_{J=|S_1-S_2|}^{S_1+S_2} \frac{A(J)}{2J+1} \sum_{J_z=-J}^{J} |J, J_z\rangle\langle J, J_z|, \tag{4.1}$$

where $A(J) \geq 0$ and $\sum_J A(J) = 1$. Entanglement structure of states under certain symmetries has been vastly explored in the literature. There are number of analytical results on the entanglement properties of $SU(2)$ invariant states. The simplest setting for analytical calculations is the $j_1 = j$, $j_2 = 1/2$ case which is characterized by a single parameter F (instead of $A(J)$). In this case, negativity has shown to be a necessary and sufficient condition and these states were found to be separable if and only if $F < 2j/(2j+1)$ [61]. Another important analytical result on the same set of states is the evaluation of entanglement of formation (EoF)

$$EoF = \begin{cases} 0, & F \in [0, 2j/(2j+1)] \\ H\left(\frac{1}{2j+1}\left(\sqrt{F} - \sqrt{2j(1-F)}\right)^2\right), & F \in [2j/(2j+1), 1], \end{cases}$$

where $H(x) = -x\log x - (1-x)\log(1-x)$ is the binary entropy [x]. One can see that entanglement goes to zero as the length of the arbitrary spin is increased, i.e. becomes more classical [x]. Extending the result on EoF to the next simplest case, two spin-1 particles, was not possible since now the most general state is characterized by two parameters which complicates the optimization procedure beyond the analytically traceable level. Although analytical formula for EoF is not present for higher dimensions, PPT criterion gives important information about the separability. For example, the case of $j_1 = j$, $j_2 \geq 1$ gives different results for integer and non-integer j; for integer j PPT is necessary and sufficient for separability, on the other hand, there are always entangled PPT states [63, 64]. Also, relative entropy of entanglement, which is upper bounded by the EoF, has been analytically calculated for $j_1 = j$, $j_2 = 1/2$ case and $j_1 = j$, $j_2 = 1$ case with integer j [65].

In real physical systems, $SU(2)$ invariant density matrices arise when, for example, considering reduced state of two spins described by a $SU(2)$ invariant Hamiltonian. There are great number of Hamiltonians that possess this symmetry, especially, in the vastly explored area of quantum spin chains [66]. Apart from those, $SU(2)$ invariant states is also present in some quantum optical setups, such as multi-photon states generated by parametric down-conversion and then undergo photon losses [67].

4.2 Quantum Discord for $j_1 = j$, $j_2 = 1/2$

We will now consider the bipartite state which is composed of a spin-j and a spin-$1/2$ subsystems. As mentioned before, in this case, we can write this state as a function of a single parameter. Density matrix for our system in total spin basis is given as [61]

$$\rho^{ab} = \frac{F}{2j}\sum_{m=-j+1/2}^{j-1/2} |j-1/2,m\rangle\langle j-1/2,m| + \frac{1-F}{2(j+1)}\sum_{m=-j-1/2}^{j+1/2} |j+1/2,m\rangle\langle j+1/2,m|. \tag{4.2}$$

To obtain an analytical formula for the quantum discord, we shall start by calculating the quantum mutual information. Bipartite density matrix has two eigenvalues $\lambda_1 = F/2j$ and $\lambda_2 = (1-F)/(2j+2)$ with degeneracies $2j$ and $2j+2$, respectively. On the other hand, the reduced density matrices of the subsystems can be found as $\rho^a = I_{2j+1}/(2j+1)$ and $\rho^b = I_2/2$ where I_{2j+1} and I_2 is the identity matrix in the dimension of the Hilbert space for spin-j and spin-$1/2$ particle, respectively. Note that both ρ^a and

ρ^b are maximally mixed independent of j. Thus the mutual information of our system is

$$\begin{aligned} I(\rho) &= S(\rho^a) + S(\rho^b) - S(\rho^{ab}) \\ &= 1 + \log_2(2j+1) + F\log_2\frac{F}{2j} + (1-F)\log_2\frac{1-F}{2j+2}. \end{aligned} \tag{4.3}$$

We now turn our attention to the calculation of the classical correlations which is the non-trivial part in our calculation. We will perform projective measurements on the spin-$1/2$ part of the density matrix. Performing POVMs complicates the calculation beyond the point of handling it analytically. In order to measure one subsystem, first we need to write the density matrix in the product basis. By using the Clebsh-Gordan coefficients for coupling a spin-j to spin-$1/2$, density matrix in product basis can be written as

$$\begin{aligned} \rho^{ab} = \frac{F}{2j}\sum_{m=-j+1/2}^{j-1/2} & a_-^2|m-1/2\rangle\langle m-1/2|\otimes|1/2\rangle\langle 1/2| \\ & + a_-b_-(|m-1/2\rangle\langle m+1/2|\otimes|1/2\rangle\langle -1/2| \\ & + |m+1/2\rangle\langle m-1/2|\otimes|-1/2\rangle\langle 1/2|) \\ & + b_-^2|m+1/2\rangle\langle m+1/2|\otimes|-1/2\rangle\langle -1/2| \\ +\frac{1-F}{2(j+1)}\sum_{m=-j-1/2}^{j+1/2} & a_+^2|m-1/2\rangle\langle m-1/2|\otimes|1/2\rangle\langle 1/2| \\ & + a_+b_+(|m-1/2\rangle\langle m+1/2|\otimes|1/2\rangle\langle -1/2| \\ & + |m+1/2\rangle\langle m-1/2|\otimes|-1/2\rangle\langle 1/2|) \\ & + b_+^2|m+1/2\rangle\langle m+1/2|\otimes|-1/2\rangle\langle -1/2|. \end{aligned} \tag{4.4}$$

Here $a_\pm = \pm\sqrt{(j+1/2\pm m)/(2j+1)}$ and $b_\pm = \sqrt{(j+1/2\mp m)/(2j+1)}$ are the appropriate Clebsh-Gordon coefficients. We want to consider the most general projective measurement which can be in any direction. So, we take the simple projectors on $+z$- and $-z$-direction and rotate then to an arbitrary direction. Explicitly, these measurement operators on ρ^b can be written as

$$\{B_k = V\Pi_k V^\dagger : k = 0, 1\}, \tag{4.5}$$

where $\{\Pi_k = |k\rangle\langle k| : k = 0, 1\}$ and $V = tI + i\vec{y}\cdot\vec{\sigma}$, any unitary matrix in SU(2). Here, both t and $\vec{y}$ are real and $t^2+y_1^2+y_2^2+y_3^2 = 1$ [40]. After the measurements are performed, ρ^{ab} will transform into an ensemble of post-measurement states with their corresponding probabilities $\{\rho_k, p_k\}$. In order to calculate possible post-measurement states ρ_k and their

corresponding probabilities p_k, we write

$$\begin{aligned} p_k\rho_k &= (I\otimes B_k)\rho^{ab}(I\otimes B_k) = (I\otimes V\Pi_k V^\dagger)\rho^{ab}(I\otimes V\Pi_k V^\dagger) \\ &= (I\otimes V)(I\otimes\Pi_k)(I\otimes V^\dagger)\rho^{ab}(I\otimes V)(I\otimes\Pi_k)(I\otimes V^\dagger). \end{aligned} \tag{4.6}$$

Since transformation of the usual Pauli matrices under V and Π_k is known [40], it is easier to calculate the post-measurement states when the spin-$1/2$ part of the density matrix is written in terms of them. In order to do that, we will use following identities

$$\begin{aligned} |1/2\rangle\langle 1/2| &= \frac{1}{2}[I+\sigma_3] \\ |1/2\rangle\langle -1/2| &= \frac{1}{2}[\sigma_1+i\sigma_2] \\ |-1/2\rangle\langle 1/2| &= \frac{1}{2}[\sigma_1-i\sigma_2] \\ |-1/2\rangle\langle -1/2| &= \frac{1}{2}[I-\sigma_3]. \end{aligned} \tag{4.7}$$

We are now ready to use the transformation properties of Pauli matrices as given in [40]

$$V^\dagger\sigma_1 V = (t^2+y_1^2-y_2^2-y_3^2)\sigma_1 + 2(ty_3+y_1y_2)\sigma_2 + 2(-ty_2+y_1y_3)\sigma_3, \tag{4.8}$$

$$V^\dagger\sigma_2 V = 2(-ty_3+y_1y_2)\sigma_1 + (t^2+y_2^2-y_1^2-y_3^2)\sigma_2 + 2(-ty_1+y_2y_3)\sigma_3, \tag{4.9}$$

$$V^\dagger\sigma_3 V = 2(ty_2+y_1y_3)\sigma_1 + 2(-ty_1+y_2y_3)\sigma_2 + (t^2+y_3^2-y_1^2-y_2^2)\sigma_3, \tag{4.10}$$

and $\Pi_0\sigma_3\Pi_0 = \Pi_0$, $\Pi_1\sigma_3\Pi_1 = -\Pi_1$, $\Pi_j\sigma_k\Pi_j = 0$ for $j=0,1$, $k=1,2$. The middle section of the second line of Eq. (4.6) can be explicitly written as

$$\begin{aligned} (I\otimes V^\dagger)\rho^{ab}(I\otimes V) = \frac{F}{2j}\sum_{m=-j+1/2}^{j-1/2} & a_-^2|m-1/2\rangle\langle m-1/2|\otimes V^\dagger|1/2\rangle\langle 1/2|V \\ & + a_-b_-(|m-1/2\rangle\langle m+1/2|\otimes V^\dagger|1/2\rangle\langle -1/2|V \\ & + |m+1/2\rangle\langle m-1/2|\otimes V^\dagger|-1/2\rangle\langle 1/2|V) \\ & + b_-^2|m+1/2\rangle\langle m+1/2|\otimes V^\dagger|-1/2\rangle\langle -1/2|V \\ \frac{1-F}{2(j+1)}\sum_{m=-j-1/2}^{j+1/2} & a_+^2|m-1/2\rangle\langle m-1/2|\otimes V^\dagger|1/2\rangle\langle 1/2|V \\ & + a_+b_+(|m-1/2\rangle\langle m+1/2|\otimes V^\dagger|1/2\rangle\langle -1/2|V \\ & + |m+1/2\rangle\langle m-1/2|\otimes V^\dagger|-1/2\rangle\langle 1/2|V) \\ & + b_+^2|m+1/2\rangle\langle m+1/2|\otimes V^\dagger|-1/2\rangle\langle -1/2|V. \end{aligned} \tag{4.11}$$

Using the identities introduced in Eq. (4.7) through Eq. (4.10), we have calculated the probabilities of obtaining two possible post-measurement states as $p_0 = p_1 = 1/2$ and the corresponding post-measurement states themselves as

$$\begin{aligned}\rho_{0_1} = \Bigg\{ & \frac{F}{2j} \sum_{m=-j+1/2}^{j-1/2} a_-^2(1+z_3)|m-1/2\rangle\langle m-1/2| \\ & \pm a_- b_-((z_1+iz_2)|m-1/2\rangle\langle m+1/2| \\ & + (z_1-iz_2)|m+1/2\rangle\langle m-1/2|) \\ & + b_-^2(1-z_3)|m+1/2\rangle\langle m+1/2| \\ & \frac{1-F}{2(j+1)} \sum_{m=-j-1/2}^{j+1/2} a_+^2(1+z_3)|m-1/2\rangle\langle m-1/2| \\ & \pm a_+ b_+((z_1+iz_2)|m-1/2\rangle\langle m+1/2| \\ & + (z_1-iz_2)|m+1/2\rangle\langle m-1/2|) \\ & + b_+^2(1-z_3)|m+1/2\rangle\langle m+1/2| \Bigg\} \otimes V\Pi_{0_1}V^\dagger,\end{aligned} \tag{4.12}$$

where $z_1 = 2(-ty_2 + y_1y_3)$, $z_2 = 2(ty_1 + y_2y_3)$, $z_3 = t^2 + y_3^2 - y_1^2 - y_2^2$ with $z_1^2 + z_2^2 + z_3^2 = 1$. In order to write the post-measurement density matrices in a more compact form, will make a couple of simplifications. These simplifications will also prove to be useful in calculating the eigenvalues of the post-measurement states. First, we take out $m = -j - 1/2$ and $m = j + 1/2$ terms out from the second summation and merge two sums. Second, we make the following observation: for an m' in the summation range we have $(|m-1/2\rangle\langle m-1/2|)|_{m'} = (|m+1/2\rangle\langle m+1/2|)|_{m'-1}$, thus we can combine their coefficients accordingly. After these modifications, the post-measurement states can be written as

$$\begin{aligned}\rho_0 = \Bigg\{ & \sum_{m=-j}^{j} \left[\frac{1}{2j+1} - z_3\frac{m(2Fj+F-j)}{j(j+1)(2j+1)}\right]|m\rangle\langle m| \\ & - (z_1+iz_2)\frac{\sqrt{j(j+1)-m(m+1)}(2Fj+F-j)}{2j(j+1)(2j+1)}|m\rangle\langle m+1| \\ & - (z_1-iz_2)\frac{\sqrt{j(j+1)-m(m+1)}(2Fj+F-j)}{2j(j+1)(2j+1)}|m+1\rangle\langle m| \Bigg\} \otimes V\Pi_0V^\dagger\end{aligned} \tag{4.13}$$

and

$$\rho_1 = \Bigg\{ \sum_{m=-j}^{j} \left[\frac{1}{2j+1} + z_3 \frac{m(2Fj+F-j)}{j(j+1)(2j+1)} \right] |m\rangle\langle m| \tag{4.14}$$
$$+ (z_1 + iz_2) \frac{\sqrt{j(j+1)-m(m+1)}(2Fj+F-j)}{2j(j+1)(2j+1)} |m\rangle\langle m+1|$$
$$+ (z_1 - iz_2) \frac{\sqrt{j(j+1)-m(m+1)}(2Fj+F-j)}{2j(j+1)(2j+1)} |m+1\rangle\langle m| \Bigg\} \otimes V\Pi_1 V^\dagger.$$

The eigenvalues of the post-measurement states are the same and by inspection, they can be found as

$$\lambda_n^{\pm} = \frac{1}{2j+1} \pm \frac{j-n}{j(j+1)(2j+1)} |(F(2j+1)-j)|, \tag{4.15}$$

where $n = 0, \cdots, \lfloor j \rfloor$ for half-integer j with $\lfloor . \rfloor$ being the floor function and $n = 0, \cdots, j$ for integer j.

In calculation of the post measurement states, we have followed the way introduced in [40]. Considering the symmetry of the states considered in this work, an alternative and a more direct way to obtain the eigenvalues of the post measurement states is present. Continuing directly from Eq. (4.6)

$$\begin{aligned} p_k \rho_k &= (I \otimes V\Pi_k V^\dagger) \rho^{ab} (I \otimes V\Pi_k V^\dagger) \\ &= (I \otimes V\Pi_k V^\dagger)(V \otimes V) \rho^{ab} (V^\dagger \otimes V^\dagger)(I \otimes V\Pi_k V^\dagger) \\ &= (I \otimes V\Pi_k)(V \otimes I) \rho^{ab} (V^\dagger \otimes I)(I \otimes \Pi_k V^\dagger) \\ &= (V \otimes V\Pi_k) \rho^{ab} (V^\dagger \otimes \Pi_k V^\dagger) \\ &= (V \otimes V)(I \otimes \Pi_k) \rho^{ab} (I \otimes \Pi_k)(V^\dagger \otimes V^\dagger). \end{aligned} \tag{4.16}$$

We only need the eigenvalues of the post-measurement states and the eigenvalues of a matrix does not change under local unitary operations. Therefore, it is sufficient for us to calculate the eigenvalues of $(I \otimes \Pi_k) \rho^{ab} (I \otimes \Pi_k)$. Applying the projection operators to the spin-$1/2$ part of the density matrix we get

$$(I \otimes \Pi_0) \rho^{ab} (I \otimes \Pi_0) = \frac{F}{2j} \sum_{m=-j+1/2}^{j-1/2} a_-^2 |m-1\rangle\langle m-1| + \frac{1-F}{2(j+1)} \sum_{m=-j-1/2}^{j+1/2} a_+^2 |m-1\rangle\langle m-1| \tag{4.17}$$

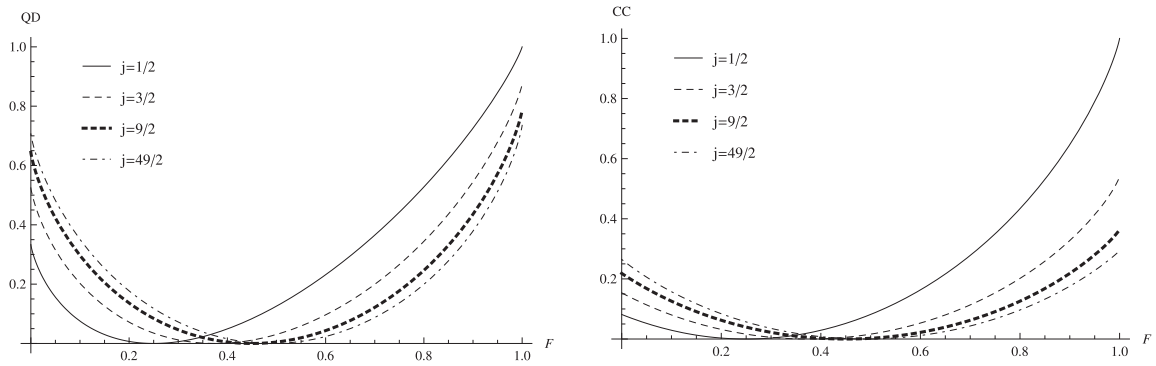

Figure 4.1: On the left panel QD vs. F and on the right panel CC vs. F for $j = 1/2$ $(d = 2)$, $j = 3/2$ $(d = 4)$, $j = 9/2$ $(d = 10)$ and $j = 49/2$ $(d = 50)$.

and

$$(I\otimes\Pi_1)\rho^{ab}(I\otimes\Pi_1) = \frac{F}{2j}\sum_{m=-j+1/2}^{j-1/2} b_-^2|m-1\rangle\langle m-1| + \frac{1-F}{2(j+1)}\sum_{m=-j-1/2}^{j+1/2} b_+^2|m-1\rangle\langle m-1|. \tag{4.18}$$

Since both of these matrices are diagonal and free of measurement parameters, it is straightforward to calculate the eigenvalues and eventually, the QD of these states. The eigenvalues obtained from these post measurement states are equivalent to the ones presented in Eq (4.15). This alternative method is especially important because it points a way to generalize the calculation of QD for bipartite states of higher spin.

It can be clearly seen that that the eigenvalues do not depend on the measurement parameters. Therefore, calculation of the classical correlations do not require any optimization over the projective measurements. Then, the classical correlations can be written as

$$C(\rho^{ab}) = S(\rho^a) - \sum_k p_k S(\rho_k^a) = \log_2(2j+1) + \sum_{n=0}^{j} \lambda_n^{\pm}\log_2(\lambda_n^{\pm}). \tag{4.19}$$

Combining the above equation with Eq. (4.3), we have obtained an analytical expression for QD in the system under consideration

$$D(\rho^{ab}) = 1 + F\log_2\frac{F}{2j} + (1-F)\log_2\frac{1-F}{2j+2} - \sum_{n=0}\lambda_n^{\pm}\log_2(\lambda_n^{\pm}), \tag{4.20}$$

where $\lambda_n^{\pm}$ is given at Eq (4.15). In Fig. 1, we present our results on QD and $C(\rho^{ab})$ as a function of our system parameter F for different dimensions. We recover the results obtained in [40, 68] in the special case of two spin-$1/2$ system. We know that for ρ^{ab}, the boundary between separable and entangled states is at $F_s = 2j/(2j+1)$ [61], which is half of the value that both QD and $C(\rho^{ab})$ vanish $F_d = j/(2j+1)$. One can observe that as the dimension of the system increases, both QD and $C(\rho^{ab})$ increase in the region

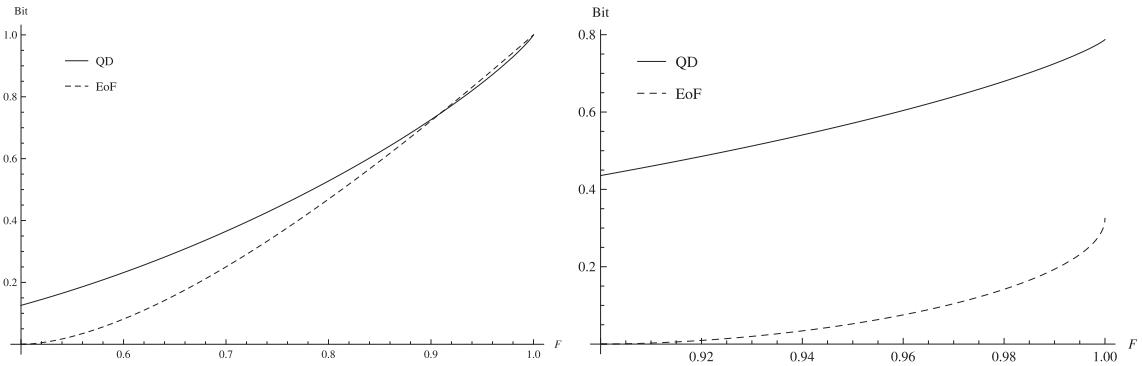

Figure 4.2: QD (solid line) and EoF (dashed line) vs. F for $j = 1/2$ ($d = 2$) (left panel) and for $j = 9/2$ ($d = 10$) (right panel)

$F < F_d$ and decrease in the region $F > F_d$. Eventually, in the infinite j limit, both of them become symmetric around the point $F = 1/2$ where they are exactly zero. The symmetry around $F = 1/2$ clearly starts to manifest itself at system dimensions as low as $j = 9/2$ ($d = 10$). The maximum value of QD is attained for $F = 1$ for all system dimensions which corresponds to the state that is the projector on to the spin-$(j - 1/2)$ subspace. It is important to note that as $j \to \infty$, our system becomes completely separable while QD remains finite except for a certain point, with its maximum value following a decreasing trend. This behavior can also be seen explicitly if we look at the large j limit of (20) as

$$D(\rho^{ab}) = 1 + F\log_2 F + (1-F)\log_2(1-F) - \log_2(2j+1) - \sum_{n=0}^{j} \Lambda_n^{\pm} \log_2 \Lambda_n^{\pm}, \quad (4.21)$$

where $\Lambda_n^{\pm} = 1/2j \pm (j-n)|(2F-1)|/(2j^2)$. The symmetry point $F = 1/2$ is apparent in the above equation and decreasing trend of the maximum value of QD can also be seen analytically as a function of j. In the same limit for $d \otimes d$ Werner states $F_s = F_d = 1/2$ and QD is again symmetric around this point. Therefore, for $QD < 1$, it is possible to find an entangled and a separable state possessing same amount of QD [46]. From the right panel of Fig. 1, it is clear that classical correlations decay in the limit $j \to \infty$. However, its maximum settles to a fairly high value as compared to $d \otimes d$ Werner states [46].

We will now compare the amount of QD and entanglement possessed in our system. EoF for a spin-$1/2$ and a spin-j $SU(2)$ invariant states is given in the beginning of this chapter. In contrast to $d \otimes d$ Werner states, the point in the parameter space for which EoF becomes non-zero is dependent on j. In [46], it was shown that EoF becomes a general upper bound for QD in $d \otimes d$ Werner states. However, in figure 2, we can see that except $j = 1/2$ case, QD always remains larger than EoF for all F and the difference between these quantities increase as $j \to \infty$. Note that the region in which EoF remains zero covers the whole parameter space in the same limit.

Chapter 5

QUANTUM CORRELATIONS IN SPIN-1 BOSE-HUBBARD MODEL

In this last chapter of the thesis, we investigate the quantum and total correlations in spin-1 Bose-Hubbard Model. Since there exists no analytical solution for arbitrary number of particles for this model, we have used analytical diagonalization technique. However, the Hilbert space dimension, i.e. the dimension of the Hamiltonian matrix to be diagonalized, grows very rapidly with increasing number of particles. Therefore, we have restricted our analysis for two and three particles. Even in this case, we obtained interesting results regarding the phases of the system via the correlation measures.

5.1 Spin-1 Bose-Hubbard Model

We will start by describing the physical setting of the system under consideration. The Hamiltonian describing the system of spin-1 atoms in an optical lattice is given by [69, 70]

$$\begin{aligned} H &= -t\sum_{\langle ij\rangle,\sigma}(a^{\dagger}_{i\sigma}a_{j\sigma}+a_{i\sigma}a^{\dagger}_{j\sigma})+\tfrac{U_0}{2}\sum_i \hat{n}_i(\hat{n}_i-1) \\ &\quad +\tfrac{U_2}{2}\sum_i((\mathbf{S}^i_{tot})^2-2\hat{n}_i), \end{aligned} \tag{5.1}$$

where $a^{\dagger}_{i\sigma}$ $(a_{i\sigma})$ is the creation (annihilation) operator for an atom on site i with z component of its spin being equal to $\sigma=-1,0,1$. Here $\hat{n}_i=\sum_\sigma a^{\dagger}_{i\sigma}a_{i\sigma}$ is the total number of atoms on site i and $\mathbf{S}^i_{tot}$ gives the total spin on ith lattice site. The parameter t represents the tunneling amplitude, U_0 is the on-site repulsion and U_2 differentiates the scattering channels between atoms with different $\mathbf{S}_{tot}$ values.

From this point on, we assume that the temperature is low enough and the tunneling amplitude t is small so that the overlap between the wavefunctions of the particles in neighboring sites is almost zero. Under these assumptions, the spin-1 Bose-Hubbard Hamiltonian can be treated perturbatively. Second order perturbation theory in t gives the

effective Hamiltonian as [70]

$$\frac{H_t^e}{t} = \omega J_z + rI + \tau \sum_{\langle ij \rangle} (\mathbf{S}_i \cdot \mathbf{S}_j) + \gamma \sum_{\langle ij \rangle} (\mathbf{S}_i \cdot \mathbf{S}_j)^2. \tag{5.2}$$

In addition to the original spin-1 Bose-Hubbard Hamiltonian, an external magnetic field ω has been added to the effective Hamiltonian. $\mathbf{S}_i$ is the spin operator of the particle on site i with $\mathbf{J} = \sum_i \mathbf{S}_i$ and I represents the identity operator. In terms of the original Bose-Hubbard Hamiltonian parameters t, U_0, U_2, the effective coupling constants r, τ, γ for single particle per site are given by

$$\begin{aligned} r &= \tfrac{4t}{3(U_0+U_2)} - \tfrac{4t}{3(U_0-2U_2)}, \\ \tau &= \tfrac{2t}{U_0+U_2}, \\ \gamma &= \tfrac{2t}{3(U_0+U_2)} + \tfrac{4t^2}{3(U_0-2U_2)}. \end{aligned} \tag{5.3}$$

with $r = \tau - \gamma$. In what follows, we will consider the two and three particle cases with a single particle per site.

5.1.1 Two particles

In this setting, the explicit form of the effective Hamiltonian given by Eq. (5.2) reads

$$H_2 = \omega J_z + rI + \tau \mathbf{S}_1 \cdot \mathbf{S}_2 + \gamma (\mathbf{S}_1 \cdot \mathbf{S}_2)^2. \tag{5.4}$$

Using the identity $\mathbf{S}_1 \cdot \mathbf{S}_2 = (J^2 - S_1^2 - S_2^2)/2$, the two particle Hamiltonian H_2 can be written in the total spin basis as

$$H_2 = \omega J_z + \frac{\tau}{2}(J^2 - 4I) + \frac{\gamma}{4}(J^2 - 4I)^2 + rI, \tag{5.5}$$

where the energy eigenvalues are determined as $E_{JM} = \omega M + \tau(j(j+1) - 2)/2 + \gamma[(j(j+1) - 4)^2 - 4]/4$. The density matrix of our system at finite temperature T can be written as

$$\rho_T = \frac{e^{-\beta H}}{Z}, \tag{5.6}$$

with the partition function of the system is given by $Z = \mathrm{tr}(e^{-\beta H}) = e^{-\beta\tau}[2\cosh\beta\tau(1 + 2\cosh\beta\omega) + e^{-\beta(3\gamma-2\tau)} + 2e^{-\beta\tau}\cosh 2\beta\tau]$ and $\beta = 1/T$ with Boltzmann constant $k_B = 1$.

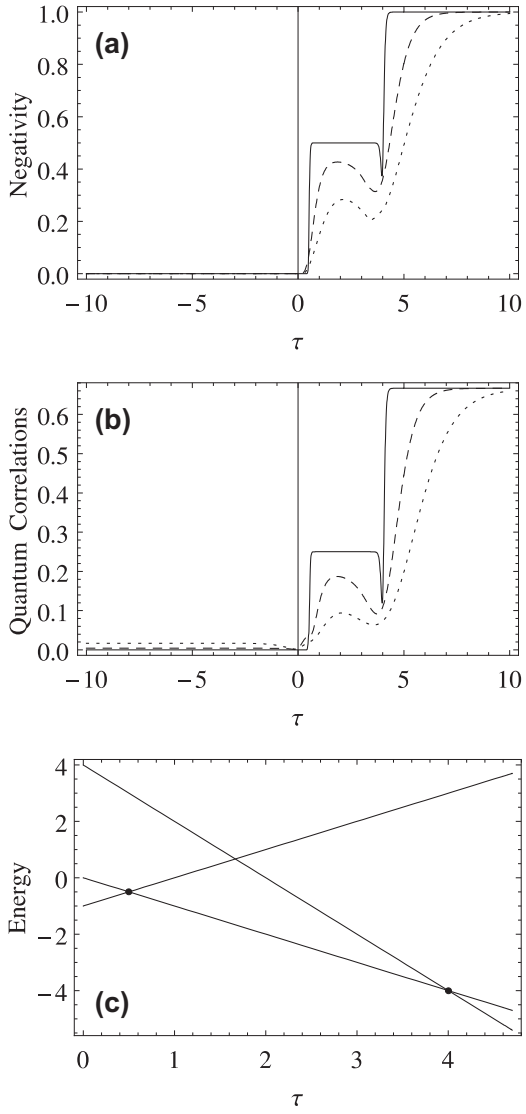

Figure 5.1: The thermal entanglement (a) and quantum correlations (b) of Spin-1 Bose-Hubbard model with two particles as a function of the parameter τ when $\gamma = \omega = 1$ for $T = 1$ (dotted line), $T = 0.5$ (dashed line) and $T = 0.05$ (solid line). The low lying energy levels and their crossings in the ground state of the system are displayed in (c).

In Fig. 5.1 (a) and (b), we present our results related to the thermal entanglement and quantum correlations in the system of two particles as a function of τ when $\gamma = \omega = 1$ for $T = 0.05, 0.5, 1$. Leggio et al. have recently discussed the behavior of thermal entanglement in this model, revealing a connection between the different phases of entanglement and the energy level crossings in the ground state of the system [71]. We demonstrate here that not only the negativity but also the non-classical correlations of the system experience two sharp transitions at points $\tau = 0.5$ and $\tau = 4$ when the temperature is sufficiently low. Examining the Fig. 5.1 (c), it is not difficult to see that these sharp transitions are connected with the appearance of energy level crossings in the ground state of the system.

In fact, ground state crossings occur at the points $2\tau = \omega$ and $\tau = \omega + 3\gamma$, and the connection between the crossings and the considered correlation measures is independent of the values of γ and ω. We also note that when $\tau < 0$, non-classical correlations in the system grows and reaches to a constant value in this regime as the temperature is increased.

5.1.2 Three particles

When it comes three particles, the effective Hamiltonian with periodic boundary conditions takes the form

$$\begin{aligned} H_3 &= \omega J_z + rI + \tau(\mathbf{S}_1 \cdot \mathbf{S}_2 + \mathbf{S}_2 \cdot \mathbf{S}_3 + \mathbf{S}_3 \cdot \mathbf{S}_1) \\ &\quad + \gamma[(\mathbf{S}_1 \cdot \mathbf{S}_2)^2 + (\mathbf{S}_2 \cdot \mathbf{S}_3)^2 + (\mathbf{S}_3 \cdot \mathbf{S}_1)^2]. \end{aligned} \tag{5.7}$$

Similarly to the case of two particles, we straightforwardly obtain the energy eigenvalues of the Hamiltonian and the thermal density matrix ρ_T to evaluate the negativity and non-classical correlations in the system. In this case, negativity and quantum correlations are calculated considering the bipartition of $3 \otimes 9$, that is, we look at the correlations between the first particle and the remaining two particles in the system. Despite the fact that we do not investigate the multipartite non-classical correlations, one can indeed use tripartite negativity defined in Ref. [72] to analyze the multipartite entanglement. It is easy to see that, due to the symmetry of the considered system, the tripartite negativity reduces to usual negativity which is calculated by taking the partial transpose with respect to any of the three qubits. Fig. 5.2 (a) and (b) display our results on the thermal entanglement and quantum correlations in the system of three particles with periodic boundary conditions as a function of τ when $\gamma = \omega = 1$ for $T = 0.05, 0.5, 1$. The low lying energy levels and their crossing points are also shown in Fig. 5.2 (c). Looking at the figures, we observe that the two sudden jumps of negativity and quantum correlations correspond to the crossings of the energy levels in the ground state of the system at $\tau = 1/3$ and $\tau = 2/3$. We note that, different from the case of two particles, negativity and quantum correlations do not show a decreasing behavior about the second transition point, $\tau = 2/3$, in case of three particles. Moreover, the plateau occurring after the first transition here is considerably shorter as compared to the two particle case. Lastly, the revival of non-classical correlations with increasing temperature can also be seen when $\tau < 0$.

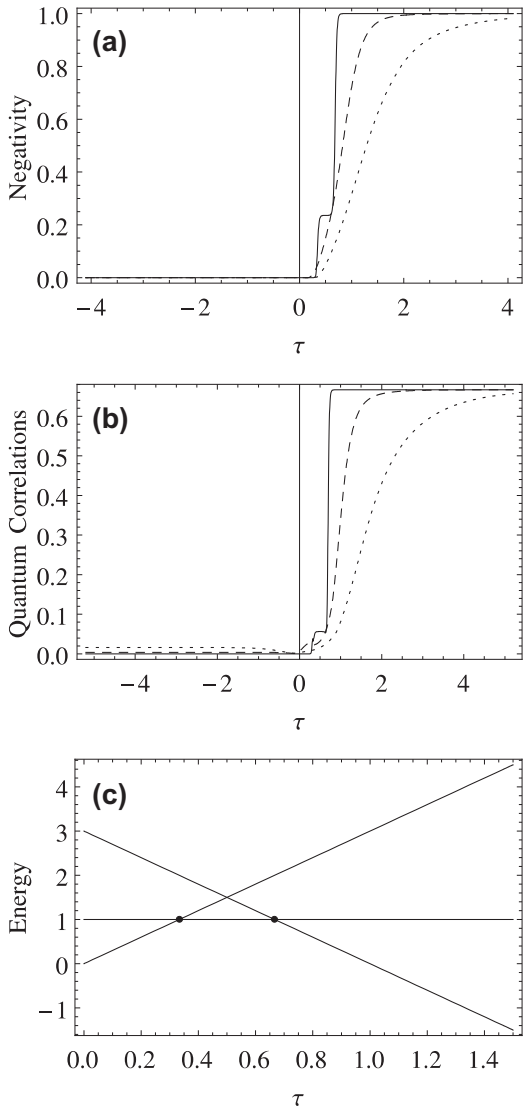

Figure 5.2: The thermal entanglement (a) and quantum correlations (b) of Spin-1 Bose-Hubbard model with three particles as a function of the parameter τ when $\gamma = \omega = 1$ for $T = 1$ (dotted line), $T = 0.5$ (dashed line) and $T = 0.05$ (solid line).The low lying energy levels and their crossings in the ground state of the system are displayed in (c).

Chapter 6

CRITICAL POINT ESTIMATION AND THERMAL CORRELATIONS IN ANISOTROPIC XY-CHAIN

In this Chapter, we will discuss the behavior of various quantum and total correlation measures both in zero and finite temperature in the anisotropic XY spin-chain. The model we are using here exhibits a quantum phase transition as one of the parameters in its Hamiltonian is varied. We will also compare the ability and success of the correlation measures to detect this critical point.

6.1 Correlations in the XY Model

Entanglement and quantum discord (QD) have been shown to identify the critical points (CPs) of QPTs with success in several different critical spin chains, both at zero [47, 66, 73–83] and finite temperature [84–86]. It has also been noted that unlike pairwise entanglement, which is typically short ranged, QD does not vanish even for distant spin pairs [76]. Another interesting aspect of quantum spin chains in transverse magnetic field is the occurrence of a non-trivial factorized ground state [87]. In order to gain a complete understanding of these factorized states, the effects of spontaneous symmetry breaking (SSB) should be considered [88–90]. In fact, concurrence is known to signal the factorization point of the anisotropic XY chain corresponding to a product ground state [90]. Moreover, it has been demonstrated that QD is also able to detect such points, provided that either SSB is taken into account or QD is calculated for different spin distances [91, 92]. In the latter case, the factorization point appears via a single intersection of the curves of QD.

We start with the analysis of the thermal quantum and total correlations in the one-dimensional XY spin chain in transverse magnetic field. The Hamiltonian of the model is

given by

$$H_{XY} = -\frac{\lambda}{2}\sum_{j=1}^{N}[(1+\gamma)\sigma_j^x\sigma_{j+1}^x + (1-\gamma)\sigma_j^y\sigma_{j+1}^y] - \sum_{j=1}^{N}\sigma_j^z \tag{6.1}$$

where N is the number of spins, σ_j^α ($\alpha = x, y, z$) is the usual Pauli operators for a spin-$1/2$ at jth site, γ ($0 \leq \gamma \leq 1$) is the anisotropy parameter and λ is the strength of the inverse external field. For $\gamma = 0$ the above Hamiltonian corresponds to the XX model. When $\gamma \geq 0$ it is in the Ising universality class, and reduces to the Ising Hamiltonian in a transverse field for $\gamma = 1$. We are interested in the region where the XY model exhibits two phases, a ferromagnetic and a paramagnetic phase, which are separated by a second-order QPT at the CP $\lambda_c = 1$. In the thermodynamic limit, the XY model can be solved exactly via a Jordan-Wigner map followed by a Bogoluibov transformation. Reduced density matrix of two spins i and j depends only on the distance between them, $r = |i - j|$, due to the translational invariance of the system. The Hamiltonian is also invariant under parity transformation, meaning it exhibits Z_2 symmetry. Taking these properties into account, and neglecting the effects of spontaneous symmetry breaking (which are studied in Ref. [88–92]), the two-spin reduced density matrix of the system is given by [73]

$$\rho_{0,r} = \frac{1}{4}[I_{0,r} + \langle\sigma^z\rangle(\sigma_0^z + \sigma_r^z)] + \frac{1}{4}\sum_{\alpha=x,y,z}\langle\sigma_0^\alpha\sigma_r^\alpha\rangle\sigma_0^\alpha\sigma_r^\alpha, \tag{6.2}$$

where $I_{0,r}$ is the four-dimensional identity matrix. The transverse magnetization is given by [93]

$$\langle\sigma^z\rangle = -\int_0^\pi \frac{(1+\lambda\cos\phi)\tanh(\beta\omega_\phi)}{2\pi\omega_\phi}d\phi, \tag{6.3}$$

where $\omega_\phi = \sqrt{(\gamma\lambda\sin\phi)^2 + (1+\lambda\cos\phi)^2}/2$, $\beta = 1/k_bT$ with k_b being the Boltzmann constant and T is the absolute temperature. Two-point correlation functions are defined as [94]

$$\langle\sigma_0^x\sigma_r^x\rangle = \begin{vmatrix} G_{-1} & G_{-2} & \cdots & G_{-r} \\ G_0 & G_{-1} & \cdots & G_{-r+1} \\ \vdots & \vdots & \ddots & \vdots \\ G_{r-2} & G_{r-3} & \cdots & G_{-1} \end{vmatrix}, \tag{6.4}$$

$$\langle \sigma_0^y \sigma_r^y \rangle = \begin{vmatrix} G_1 & G_0 & \cdots & G_{-r+2} \\ G_2 & G_1 & \cdots & G_{-r+3} \\ \vdots & \vdots & \ddots & \vdots \\ G_r & G_{r-1} & \cdots & G_1 \end{vmatrix}, \tag{6.5}$$

$$\langle \sigma_0^z \sigma_r^z \rangle = \langle \sigma^z \rangle^2 - G_r G_{-r}, \tag{6.6}$$

where

$$\begin{aligned} G_r = & \int_0^\pi \frac{\tanh(\beta\omega_\phi)\cos(r\phi)(1+\lambda\cos\phi)}{2\pi\omega_\phi} d\phi \\ & - \gamma\lambda \int_0^\pi \frac{\tanh(\beta\omega_\phi)\sin(r\phi)\sin(\phi)}{2\pi\omega_\phi} d\phi. \end{aligned} \tag{6.7}$$

6.1.1 Behavior of correlations

In Fig. 6.1, we present our results regarding the thermal total correlations quantified by MIN and WYSIM for first nearest neighbors as a function of λ for $kT = 0, 0.1, 0.5$ and $\gamma = 0.001, 0.5, 1$. We note that although MIN and WYSIM behave in a similar fashion for $\gamma = 1$, they show qualitatively different behaviors in the case of $\gamma = 0.001$. Namely, WYSIM experiences a more dramatic increase about the CP $\lambda = 1$ than MIN, and reaches to a constant value more quickly. Furthermore, it is also important to observe that as temperature increases, both of the measures cease to exhibit a non-trivial behavior about the CP.

It has been shown that QPTs can be characterized by looking at the two-spin reduced density matrix and its derivatives with respect to the tuning parameter driving the transition [66, 74]. Since correlation measures are directly determined from the reduced density matrix, they provide information about the CPs and the order of QPTs. The CP for a second-order QPT at zero temperature is signalled by a divergence or discontinuity in the first derivative of the correlation measures. If the first derivative is discontinuous, then the divergence of the second derivative pinpoints the CP [47, 66, 74]. In Fig. 6.2, we plot the derivatives of MIN and WYSIM as a function of λ for $kT = 0, 0.1, 0.5$ and $\gamma = 0.001, 0.5, 1$. We observe that both of the measures are capable of spotlighting the CP at $kT = 0$ for all values of γ. It is worth to note that with increasing temperature, the divergence at CP disappears and the peaks of the derivatives start to shift. Therefore, the measures lose their significance in determining the CP of the transition.

We now turn our attention to the analysis of thermal quantum correlations quantified by OMQC and concurrence.

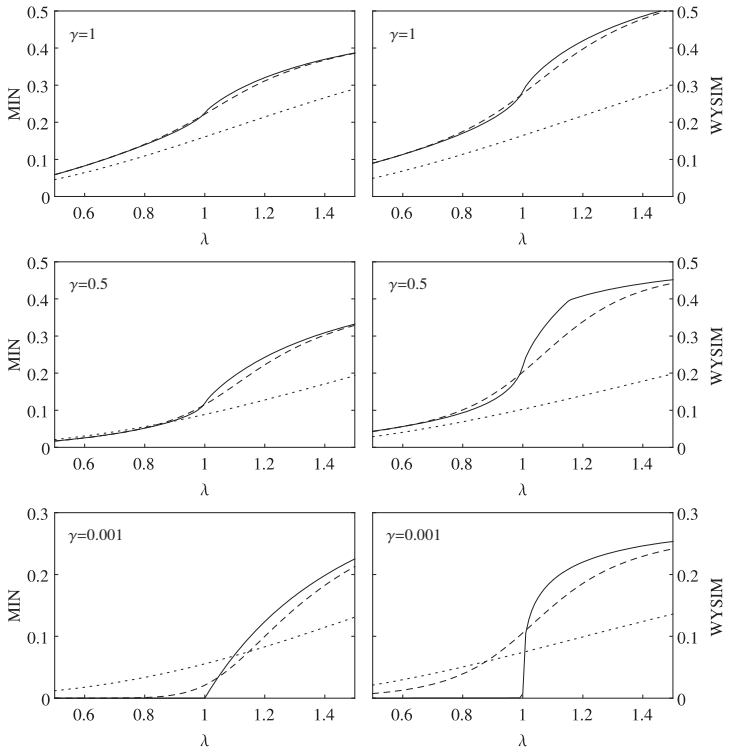

Figure 6.1: The thermal total correlations as a function of λ for $\gamma = 0.001, 0.5, 1$ at $kT = 0$ (solid line), $kT = 0.1$ (dashed line) and $kT = 0.5$ (dotted line). The graphs are for first nearest neighbors.

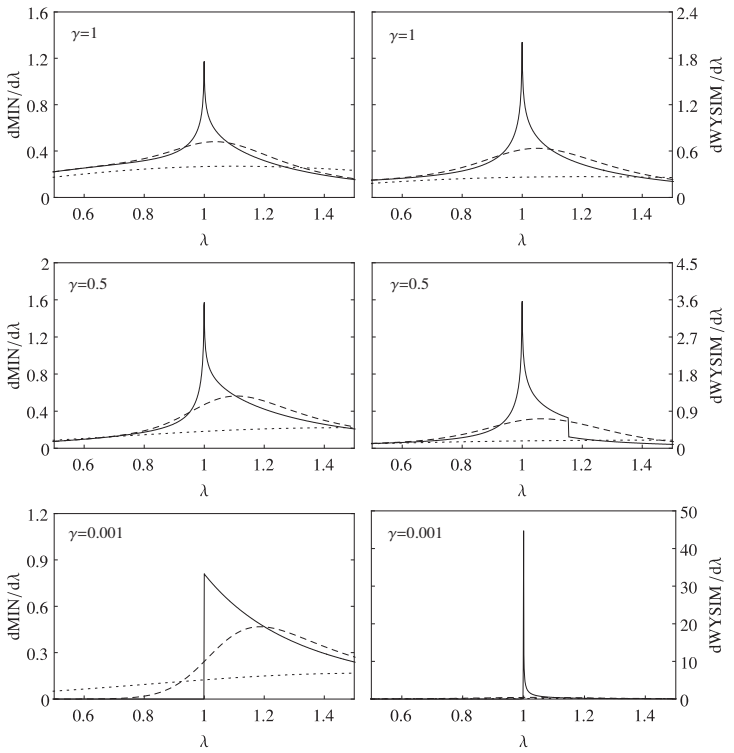

Figure 6.2: The first derivatives thermal total correlations as a function of λ for $\gamma = 0.001, 0.5, 1$ at $kT = 0$ (solid line), $kT = 0.1$ (dashed line) and $kT = 0.5$ (dotted line). The graphs are for first nearest neighbors.

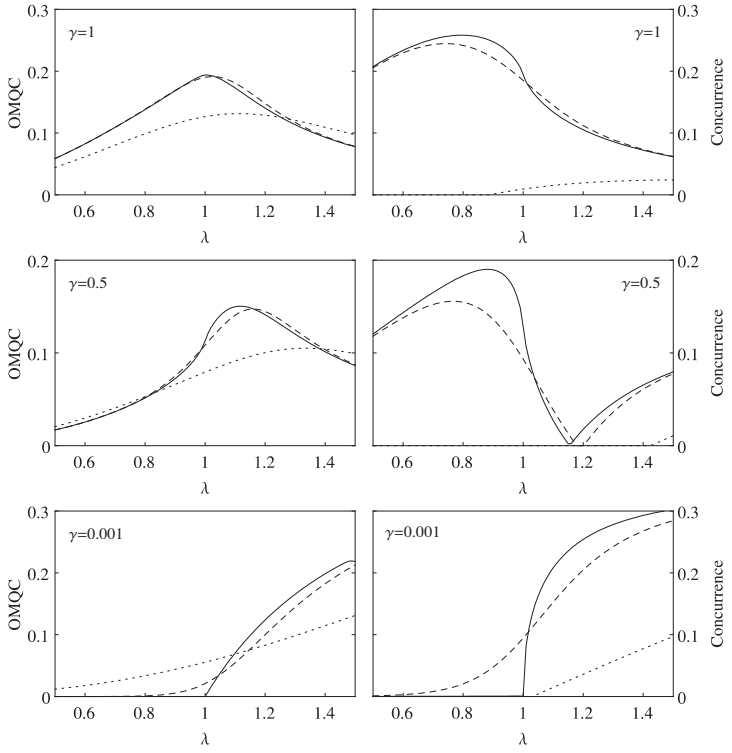

Figure 6.3: The thermal quantum correlations as a function of λ for $\gamma = 0.001, 0.5, 1$ at $kT = 0$ (solid line), $kT = 0.1$ (dashed line) and $kT = 0.5$ (dotted line). The graphs are for first nearest neighbors.

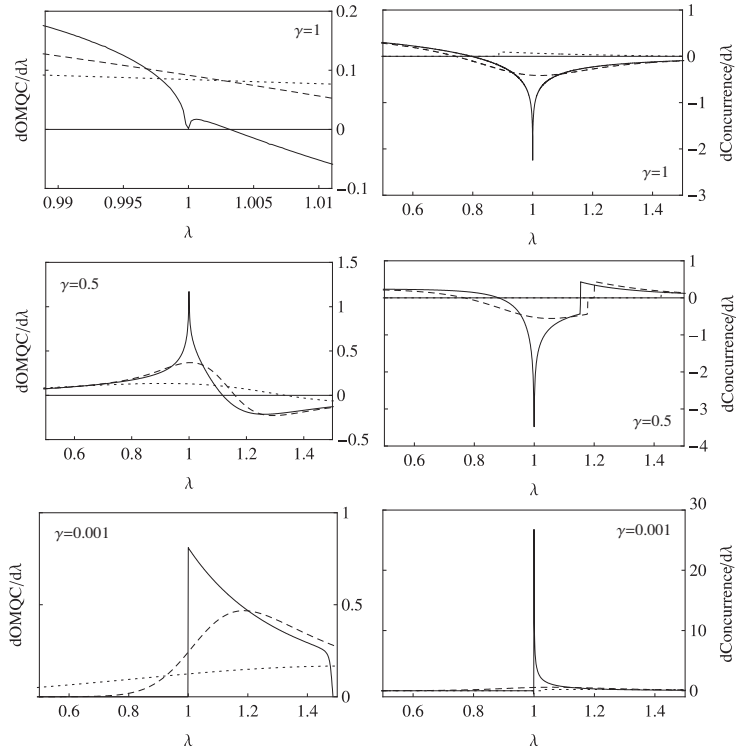

Figure 6.4: The first derivatives of thermal quantum correlations as a function of λ for $\gamma = 0.001, 0.5, 1$ at $kT = 0$ (solid line), $kT = 0.1$ (dashed line) and $kT = 0.5$ (dotted line). The graphs are for first nearest neighbors.

In Fig. 6.3 and Fig. 6.4, we plot these measures and their derivatives with respect to the driving parameter λ for first nearest neighbors as a function of λ for $kT = 0, 0.1, 0.5$. While concurrence suffers a drastic decrease as temperature increases, OMQC still captures significant amount of correlation, making it more robust against thermal effects. It can also be seen that at $kT = 0$ the CP can be detected by analyzing the non-analyticities in the first derivatives of the measures. The fact that there exists a relation between the appearance of a divergence in the derivatives of the correlation measures of the ground state and the occurrence of the QPT can be understood within a general framework developed by Wu *et al*. [74]. The energy of two spins at the sites i and j is given by

$$E(\rho_{ij}) = \sum_{ij} \mathrm{Tr}\left\{H_{ij}\rho_{ij}\right\}, \tag{6.8}$$

where ρ_{ij} is the reduced density matrix of the spins and H_{ij} is their reduced Hamiltonian whose summation over all sites restores the full Hamiltonian of the chain, $\sum_{ij} H_{ij} = H$. It is straightforward to obtain the first two derivatives of the two-site energy given by Eq. (6.8) with respect to the field λ as

$$\begin{aligned} \frac{\partial E(\rho_{ij})}{\partial \lambda} &= \sum_{ij} \mathrm{Tr}\left\{\frac{\partial H_{ij}}{\partial \lambda}\rho_{ij}\right\}, \\ \frac{\partial^2 E(\rho_{ij})}{\partial \lambda^2} &= \sum_{ij} \left[\mathrm{Tr}\left\{\frac{\partial^2 H_{ij}}{\partial \lambda^2}\rho_{ij}\right\} + \mathrm{Tr}\left\{\frac{\partial H_{ij}}{\partial \lambda}\frac{\partial \rho_{ij}}{\partial \lambda}\right\}\right]. \end{aligned} \tag{6.9}$$

Considering that the derivatives of the reduced Hamiltonian are continuous with respect to the magnetic field λ, we realize that possible discontinuities in the derivatives of ground state energy have their roots at the elements of the reduced density matrices ρ_{ij}. Specifically, whereas a discontinuity in the first derivative of the ground state energy (a first order QPT) hints at a discontinuity in at least one of the elements of the reduced density matrix ρ_{ij}, a discontinuity or divergence in the second derivative of the ground state energy (a second order QPT) suggests a divergence of at least one of the elements of the derivative of the reduced density matrix $\partial\rho_{ij}/\partial\lambda$. Having this discussion in mind, it is rather straightforward to comprehend why two-spin or even single-spin coherence might be sufficient to pinpoint the CP of the QPT. However, it is very important to note that such a correspondence between the non-analyticities in physical quantities, that are functions of the reduced density matrix elements, and the CPs of QPTs does not always hold. Depending on the mathematical properties of the considered quantity (correlation measures, coherence measures, etc.), it is possible that the CP of a QPT is not caught by a measure due to some unlucky coincidences.

Next, we discuss the question of whether the studied correlation measures can signal

the emergence of non-trivial product ground state in the XY spin chain. Despite the fact that the ground state of the model is entangled in general, for some special values of γ and λ, the ground state becomes completely factorized. In particular, except the trivial factorization points $\lambda = 0$ and $\lambda \to \infty$, there also exists a non-trivial factorization line corresponding to $\gamma^2 + \lambda^{-2} = 1$. Accordingly, as can seen from the behavior of concurrence in Fig. 6.3 for $\gamma = 0.5$, entanglement vanishes at $\lambda \simeq 1.15$, which spotlights the occurrence of a product ground state. It is shown in Fig. 6.2 that, unlike OMQC and MIN, WYSIM can signal this factorization point through a non-analytical behavior in its derivative. For QD to identify this point when the distance between the spins is fixed, the effects of SSB must be taken into account [91, 92, 95]. Therefore, it is important to recognize that the calculation of WYSIM between the spins at a fixed distance enables us to detect the product ground state even in the absence of SSB.

6.1.2 Critical point estimation at finite temperatures

Having discussed the behaviors of the thermal total and quantum correlations, we now explore the ability of these measures to correctly estimate the CP of the QPT at finite temperature. Despite the disappearance of the singular behavior of MIN, WYSIM, OMQC and concurrence with increasing temperature, it might still be possible to estimate the CP at finite temperature [86]. For sufficiently low temperatures, divergent behaviors of the first derivatives of correlation measures at $T = 0$ will be replaced by a local maximum or minimum about the CP. Therefore, in order to estimate the CP, we search for this extremum point. On the other hand, a discontinuous first derivative at $T = 0$ requires us to look for an extremum point in the second derivative for $T > 0$. In Fig. 6.5, we present the results of our analysis regarding the estimation of CP as a function of kT for first and second nearest neighbors when $\gamma = 0.001, 0.5, 1$. Before starting to compare the ability of MIN, WYSIM, OMQC and concurrence to indicate the CP in detail, we notice that the success rates of these measures strongly depend on the anisotropy parameter of the Hamiltonian. In the case of first nearest neighbors, at $\gamma = 1$, all of the correlation measures are able to predict the CP reliably, with concurrence being the most effective among them. When $\gamma = 0.5$ MIN turns out to be the worst CP estimator. While WYSIM and concurrence points out the CP relatively well as compared to MIN, OMQC clearly outperforms all others and estimates the CP in a exceptionally accurate way. For $\gamma = 0.001$, MIN and OMQC become identical, and they predict the location of the CP significantly worse than WYSIM and concurrence.

For second nearest neighbors, even though we do not present the graphs of correlation

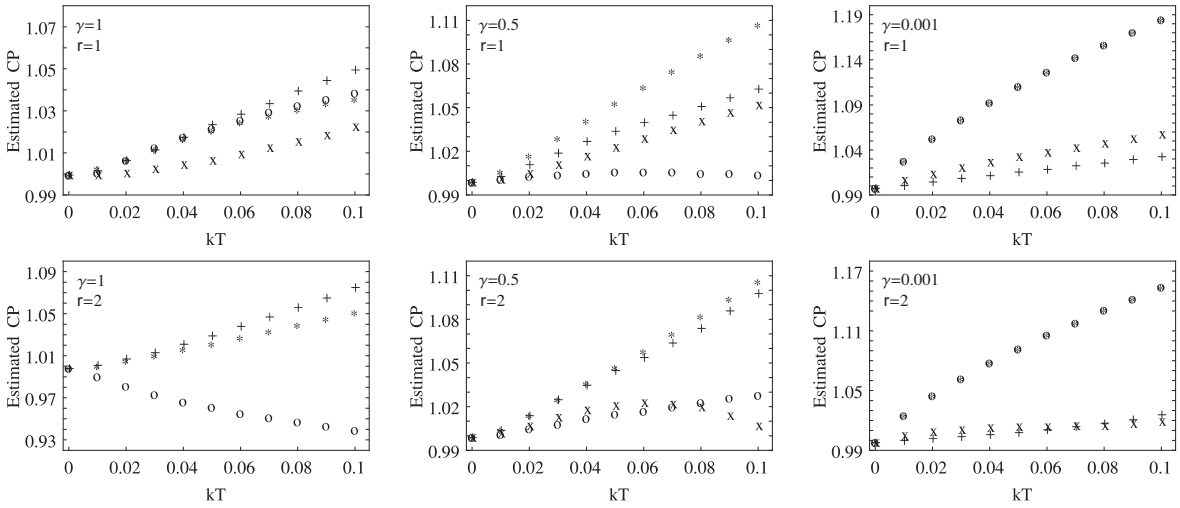

Figure 6.5: The estimated values of the CP as a function of kT for three different values of the anisotropy parameter $\gamma = 0.001, 0.5, 1$. The CPs in the graphs are estimated by OMQC (denoted by o), WYSIM (denoted by +), MIN (denoted by $*$) and concurrence (denoted by x). Concurrence is not included for $\gamma = 1$ and $r = 2$, since it vanishes at even very low temperatures.

measures and their derivatives, the CP has been inspected by performing the same analysis as in the first nearest neighbor case. The CPs estimated by WYSIM, OMQC and MIN for $\gamma = 1$ deviate from the true CP by the same amount but they are still acceptable. In the case of $\gamma = 0.5$, both concurrence and OMQC estimate the CP very well in contrast to WYSIM and MIN. Finally, when $\gamma = 0.001$, while WYSIM and concurrence spotlight the CP remarkably well, OMQC and MIN perform very poorly. It is also worth to notice that concurrence performs even better than the first nearest neighbors case for $\gamma = 0.5$ and $\gamma = 0.001$.

Furthermore, the ability of entanglement of formation (EOF) and QD to estimate the CP of the XY spin chain at finite temperature has been recently studied by Werlang et al. [86]. The performance of the correlations measures used in this work as compared to QD and EOF depend on the anisotropy parameter of the Hamiltonian and also on the distance between the spin pairs. For instance, in the first nearest neighbors case at $\gamma = 0.5$, among the correlation measures considered here, only OMQC performs as well as QD and EOF. On the other hand, for the second nearest neighbors at $\gamma = 0.001$, while WYSIM and concurrence turn out to be better CP estimators than QD and EOF, MIN and OMQC do not perform as well. We lastly note that apart from a limited number of special cases, QD still proves to be the most accurate CP estimator for the anisotropic XY spin chain.

6.1.3 Long-range correlations

Inspired by the methods of Ref. [79], we now examine the long-range behavior of the thermal total and quantum correlations for the one-dimensional XY model in transverse magnetic field. While entanglement vanishes for distant spin pairs even in the ordered ferromagnetic phase, QD has been shown to remain non-zero [76, 79]. Fig. 6.6 demonstrates our results related to the dependence of MIN, WYSIM and OMQC on the distance between the spin pairs at finite temperature, for $\lambda = 0.75, 0.95, 1.05, 1.5$ and $\gamma = 0.001, 1$. In case of $\gamma = 0.001$, neither of the correlation measures remain significant when the distance between the spin pairs is increased. We can also see that the decay of the correlations hasten when the temperature rises. For the Ising model limit ($\gamma = 1$), even though MIN, WYSIM and OMQC approach to a finite value in the ordered phase for sufficiently low temperatures, thermal effects wipe out the correlations between distant spin pairs after a certain temperature.

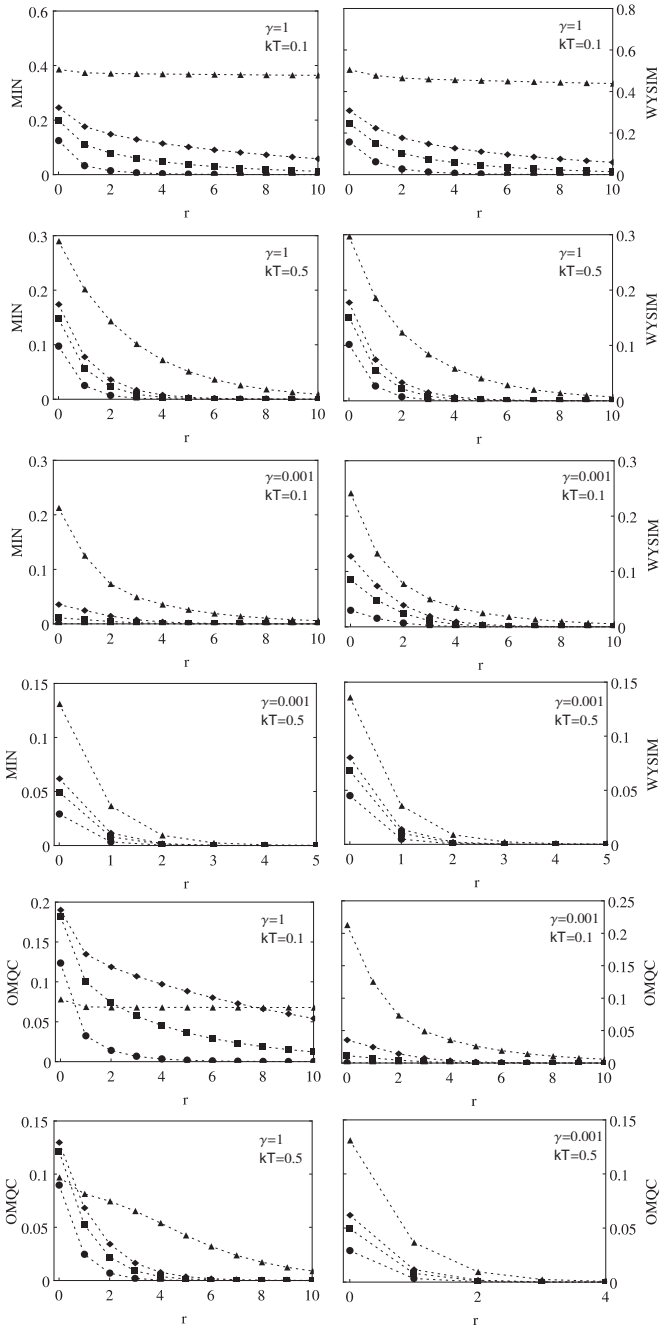

Figure 6.6: Long-range behavior of the thermal total and quantum correlations for $\gamma = 0.001$ and $\gamma = 1$ at $kT = 0.1, 0.5$. The circles, squares, diamonds and triangles correspond to $\lambda = 0.75$, $\lambda = 0.95$, $\lambda = 1.05$ and $\lambda = 1.5$, respectively.

Chapter 7

CONCLUSION

In this thesis, we have analytically calculated the quantum discord for the $SU(2)$-invariant systems consisting of spin-j and spin-$1/2$ and presented a recipe to generalize the calculation to arbitrary spin subsystems. Furthermore, we have investigated various measures of quantum and total correlations in anisotropic XY spin-chain and in few-atom spin-1 Bose-Hubbard model. The main results presented in Chapters 3 to 5 were also published in three different papers.

In Chapter 2, we have analytically calculated the QD of a $SU(2)$ invariant system, consisting of a spin-j and a spin-$1/2$ subsystems. We have compared our results with entanglement structure of these systems and QD of states having similar symmetries. It is known that a very small subset of the set of states addressed in this work possess entanglement as the dimension of the spin-j particle becomes larger. We have shown that in the large j limit, QD remains significantly larger than the entanglement. On the other hand, we have seen that maximum value of QD decreases with the increasing system size. We have also suggested a way to generalize the calculation for bipartite spins of arbitrary magnitude. Observation of $SU(2)$ invariant states in many real physical systems, make them a good candidate for utilization in quantum computing protocols that rely on QD.

In the third chapter, we have investigated the thermal quantum correlations and entanglement in a spin-1 Bose-Hubbard model with two and three particles with periodic boundary conditions. Our results demonstrate that both the behavior of thermal quantum correlations and entanglement spotlight the energy level crossings in the ground state of the system. Despite the fact that our discussion is limited to few particle systems, the connection between the behavior of correlations measures and ground state crossings might have consequences even for real quantum critical systems having large number of particles. Finally, we suggest that it would be interesting to analyze the relation of some thermodynamical quantities (such as the specific heat) and correlations measures since various non-trivial behaviors of certain thermodynamical quantities might give information about the correlations in the system.

In the fourth and final chapter, we have discussed the thermal quantum and total correlations in the one-dimensional anisotropic XY model in transverse magnetic field from several perspectives. We have quantified the correlations using recently proposed correlation measures such as WYSIM, MIN and OMQC, and a well known entanglement measure concurrence. Analyzing these measures in the parameter space of the Hamiltonian for first and second nearest neighbors, we have found that all of the considered measures are capable of indicating the CP of the transition. Although the interesting behavior of the measures in the vicinity of the CP disappears as the temperature increases, for sufficiently low temperatures, it is still possible to estimate the CP by looking at the derivatives of the correlation measures. We have observed that the ability of the measures to predict the CP strongly depend on the anisotropy parameter γ. For instance, while OMQC spotlights the CP with a remarkably high accuracy at $\gamma = 0.5$ for first nearest neighbors, it performs very poorly at $\gamma = 0.001$. On the other hand, WYSIM points out the CP reasonably well at $\gamma = 0.001$ for both first and second neighbors. Moreover, we have shown that, among the new measures considered in this work, only WYSIM is able to identify the factorization point of the XY spin chain even if we disregard the effects of SSB. These results demonstrate for the first time that OMQC and WYSIM are relevant quantities for identifying CPs in concrete physical problems. Next, we have investigated how WYSIM, MIN and OMQC are affected as we increase the distance between spin pairs. We have found that the case of $\gamma = 0.001$ is more susceptible to both increasing distance of spin pairs and thermal effects.

Bibliography

[1] R. Horodecki, P. Horodecki, M. Horodecki, and K. Horodecki, "Quantum entanglement," *Reviews of Modern Physics*, vol. 81, pp. 865–942, 2009.

[2] L. Amico, R. Fazio, A. Osterloh, and V. Vedral, "Entanglement in many-body systems," *Reviews of Modern Physics*, vol. 80, pp. 517–576, 2008.

[3] L. Henderson and V. Vedral, "Classical, quantum and total correlations," *Journal of Physics A: Mathematical and General*, vol. 34, no. 35, p. 6899, 2001.

[4] H. Ollivier and W. H. Zurek, "Quantum discord: a measure of the quantumness of correlations," *Physical Review Letters*, vol. 88, p. 017901, 2001.

[5] A. Datta, A. Shaji, and C. M. Caves, "Quantum discord and the power of one qubit," *Physical Review Letters*, vol. 100, p. 050502, 2008.

[6] E. Knill and R. Laflamme, "Power of one bit of quantum information," *Physical Review Letters*, vol. 81, pp. 5672–5675, 1998.

[7] K. Modi, A. Brodutch, H. Cable, T. Paterek, and V. Vedral, "The classical-quantum boundary for correlations: discord and related measures," *Reviews of Modern Physics*, vol. 84, pp. 1655–1707, 2012.

[8] S. Sachdev, *Quantum Phase Transitions*. Cambridge University Press, 2001.

[9] S. Hill and W. K. Wootters, "Entanglement of a pair of quantum bits," *Physical Review Letters*, vol. 78, pp. 5022–5025, 1997.

[10] W. K. Wootters, "Entanglement of formation of an arbitrary state of two qubits," *Physical Review Letters*, vol. 80, pp. 2245–2248, 1998.

[11] D. Girolami and G. Adesso, "Observable measure of bipartite quantum correlations," *Physical Review A*, vol. 108, p. 150403, 2012.

[12] B. Dakić, V. Vedral, and C. Brukner, "Necessary and sufficient condition for nonzero quantum discord," *Physical Review Letters*, vol. 105, p. 190502, 2010.

[13] S. Luo and S. Fu, "Measurement-induced nonlocality," *Physical Review Letters*, vol. 106, p. 120401, 2011.

[14] S. Luo, S. Fu, and C. H. Oh, "Quantifying correlations via the Wigner-Yanase skew information," *Physical Review A*, vol. 85, p. 032117, 2012.

[15] T. Zhou, J. Cui, and G. L. Long, "Measure of nonclassical correlation in coherence-vector representation," *Physical Review A*, vol. 84, p. 062105, 2011.

[16] D. Griffiths, *Introduction to quantum mechanics*. Pearson Prentice Hall, 2005.

[17] J. Sakurai and J. Napolitano, *Modern quantum mechanics*. Addison-Wesley, 2010.

[18] E. Merzbacher, *Quantum mechanics*. John Wiley and Sons, 3rd ed., 1998.

[19] R. Shankar, *Principles of quantum mechanics*. Springer, 1994.

[20] K. Gottfried and T. Yan, *Quantum mechanics: fundamentals*. Springer, 2003.

[21] A. Peres, *Quantum theory: concepts and methods*. Springer, 1995.

[22] M. Nielsen and I. Chuang, *Quantum computation and quantum information*. Cambridge University Press, 2000.

[23] L. Diósi, *A short course in quantum information theory: an approach from theoretical physics*. Springer, 2007.

[24] R. F. Werner, "Quantum states with Einstein-Podolsky-Rosen correlations admitting a hidden-variable model," *Physical Review A*, vol. 40, pp. 4277–4281, 1989.

[25] A. Peres, "Separability criterion for density matrices," *Physical Review Letters*, vol. 77, pp. 1413–1415, 1996.

[26] M. Horodecki, P. Horodecki, and R. Horodecki, "Separability of mixed states: necessary and sufficient conditions," *Physics Letters A*, vol. 223, no. 1–2, pp. 1–8, 1996.

[27] C. H. Bennett, G. Brassard, S. Popescu, B. Schumacher, J. A. Smolin, and W. K. Wootters, "Purification of noisy entanglement and faithful teleportation via noisy channels," *Physical Review Letters*, vol. 76, pp. 722–725, 1996.

[28] C. H. Bennett, H. J. Bernstein, S. Popescu, and B. Schumacher, "Concentrating partial entanglement by local operations," *Physical Review A*, vol. 53, pp. 2046–2052, 1996.

[29] C. H. Bennett, D. P. DiVincenzo, J. A. Smolin, and W. K. Wootters, "Mixed-state entanglement and quantum error correction," *Phys. Rev. A*, vol. 54, pp. 3824–3851, Nov 1996.

[30] C. H. Bennett, S. Popescu, D. Rohrlich, J. A. Smolin, and A. V. Thapliyal, "Exact and asymptotic measures of multipartite pure-state entanglement," *Physical Review A*, vol. 63, p. 012307, 2000.

[31] M. Horodecki, "Entanglement measures," *Quantum Information and Computation*, vol. 1, pp. 3–26, 2001.

[32] V. Vedral, M. B. Plenio, M. A. Rippin, and P. L. Knight, "Quantifying entanglement," *Physical Review Letters*, vol. 78, pp. 2275–2279, 1997.

[33] V. Vedral and M. B. Plenio, "Entanglement measures and purification procedures," *Physical Review A*, vol. 57, pp. 1619–1633, 1998.

[34] M. B. Plenio, "Logarithmic negativity: a full entanglement monotone that is not convex," *Physical Review Letters*, vol. 95, p. 090503, 2005.

[35] M. B. Plenio and S. Virmani, "An introduction to entanglement measures," *Quantum Information and Computation*, vol. 7, pp. 1–51, 2007.

[36] G. Vidal, "Entanglement monotones," *Journal of Modern Optics*, vol. 47, no. 2–3, pp. 355–376, 2000.

[37] C. Shannon, "A mathematical theory of communication," *The Bell System Technical Journal*, vol. 27, pp. 379–423,623–656, 1948.

[38] S. Popescu and D. Rohrlich, "Thermodynamics and the measure of entanglement," *Physical Review A*, vol. 56, pp. R3319–R3321, 1997.

[39] G. Vidal and R. F. Werner, "Computable measure of entanglement," *Physical Review A*, vol. 65, p. 032314, 2002.

[40] S. Luo, "Quantum discord for two-qubit systems," *Physical Review A*, vol. 77, p. 042303, 2008.

[41] M. Ali, A. R. P. Rau, and G. Alber, "Quantum discord for two-qubit X states," *Physical Review A*, vol. 81, p. 042105, 2010.

[42] Q. Chen, C. Zhang, S. Yu, X. X. Yi, and C. H. Oh, "Quantum discord of two-qubit X states," *Physical Review A*, vol. 84, p. 042313, 2011.

[43] S. Vinjanampathy and A. R. P. Rau, "Quantum discord for qubit-qudit systems," *Journal of Physics A: Mathematical and Theoretical*, vol. 45, no. 9, p. 095303, 2012.

[44] D. Girolami and G. Adesso, "Quantum discord for general two-qubit states: Analytical progress," *Phys. Rev. A*, vol. 83, p. 052108, May 2011.

[45] M. Ali, "Quantum discord for a two-parameter class of states in $2 \times d$ quantum systems," *Journal of Physics A: Mathematical and Theoretical*, vol. 43, no. 49, p. 495303, 2010.

[46] E. Chitambar, "Quantum correlations in high-dimensional states of high symmetry," *Phys. Rev. A*, vol. 86, p. 032110, Sep 2012.

[47] M. S. Sarandy, "Classical correlation and quantum discord in critical systems," *Physical Review A*, vol. 80, p. 022108, 2009.

[48] G. Adesso and A. Datta, "Quantum versus classical correlations in Gaussian states," *Physical Review Letters*, vol. 105, p. 030501, 2010.

[49] L.-X. Cen, X.-Q. Li, J. Shao, and Y. Yan, "Quantifying quantum discord and entanglement of formation via unified purifications," *Physical Review A*, vol. 83, p. 054101, 2011.

[50] F. Galve, G. L. Giorgi, and R. Zambrini, "Maximally discordant mixed states of two qubits," *Physical Review A*, vol. 83, p. 012102, 2011.

[51] F. Lastra, C. E. López, L. Roa, and J. C. Retamal, "Entanglement of formation for a family of (2$\bigotimes$d)-dimensional systems," *Phys. Rev. A*, vol. 85, p. 022320, Feb 2012.

[52] B. Bylicka and D. Chruściński, "Witnessing quantum discord in (2$\bigotimes$n) systems," *Phys. Rev. A*, vol. 81, p. 062102, Jun 2010.

[53] B. Bellomo, G. L. Giorgi, F. Galve, R. Lo Franco, G. Compagno, and R. Zambrini, "Unified view of correlations using the square-norm distance," *Phys. Rev. A*, vol. 85, p. 032104, Mar 2012.

[54] S. Luo, "Using measurement-induced disturbance to characterize correlations as classical or quantum," *Physical Review A*, vol. 77, p. 022301, 2008.

[55] S. Luo and S. Fu, "Geometric measure of quantum discord," *Physical Review A*, vol. 82, p. 034302, 2010.

[56] M. Gessner, E.-M. Laine, H.-P. Breuer, and J. Piilo, "Correlations in quantum states and the local creation of quantum discord," *Phys. Rev. A*, vol. 85, p. 052122, May 2012.

[57] A. Streltsov, H. Kampermann, and D. Bruß, "Behavior of quantum correlations under local noise," *Phys. Rev. Lett.*, vol. 107, p. 170502, Oct 2011.

[58] X. Hu, H. Fan, D. L. Zhou, and W.-M. Liu, "Necessary and sufficient conditions for local creation of quantum correlation," *Phys. Rev. A*, vol. 85, p. 032102, Mar 2012.

[59] F. Ciccarello and V. Giovannetti, "Creating quantum correlations through local nonunitary memoryless channels," *Phys. Rev. A*, vol. 85, p. 010102, Jan 2012.

[60] E. P. Wigner and M. M. Yanase, "Information contents of distributions," *Proceedings of the National Academy of Sciences of the United States of America*, vol. 49, pp. 910–918, 1963.

[61] J. Schliemann, "Entanglement in su(2)-invariant quantum spin systems," *Phys. Rev. A*, vol. 68, p. 012309, Jul 2003.

[62] J. Schliemann, "Entanglement in su(2)-invariant quantum systems: The positive partial transpose criterion and others," *Phys. Rev. A*, vol. 72, p. 012307, Jul 2005.

[63] H.-P. Breuer, "State space structure and entanglement of rotationally invariant spin systems," *Journal of Physics A: Mathematical and General*, vol. 38, no. 41, p. 9019, 2005.

[64] H.-P. Breuer, "Entanglement in so(3)-invariant bipartite quantum systems," *Phys. Rev. A*, vol. 71, p. 062330, Jun 2005.

[65] Z. Wang and Z. Wang, "Relative entropy of entanglement of rotationally invariant states," *Physics Letters A*, vol. 372, no. 47, pp. 7033 – 7037, 2008.

[66] R. Dillenschneider, "Quantum discord and quantum phase transition in spin chains," *Physical Review B*, vol. 78, p. 224413, 2008.

[67] G. A. Durkin, C. Simon, J. Eisert, and D. Bouwmeester, "Resilience of multiphoton entanglement under losses," *Phys. Rev. A*, vol. 70, p. 062305, Dec 2004.

[68] F. F. Fanchini, T. Werlang, C. A. Brasil, L. G. E. Arruda, and A. O. Caldeira, "Non-markovian dynamics of quantum discord," *Phys. Rev. A*, vol. 81, p. 052107, May 2010.

[69] I. Bloch, J. Dalibard, and W. Zwerger, "Many-body physics with ultracold gases," *Rev. Mod. Phys.*, vol. 80, pp. 885–964, Jul 2008.

[70] A. Imambekov, M. Lukin, and E. Demler, "Spin-exchange interactions of spin-one bosons in optical lattices: Singlet, nematic, and dimerized phases," *Phys. Rev. A*, vol. 68, p. 063602, Dec 2003.

[71] B. Leggio, A. Napoli, and A. Messina, "Entanglement and heat capacity in a two-atom bose-hubbard model," *Physics Letters A*, vol. 376, no. 4, pp. 339 – 343, 2012.

[72] C. Sabín and G. García-Alcaine, "A classification of entanglement in three-qubit systems," *The European Physical Journal D*, vol. 48, no. 3, pp. 435–442, 2008.

[73] T. J. Osborne and M. A. Nielsen, "Entanglement in a simple quantum phase transition," *Physical Review A*, vol. 66, p. 032110, 2002.

[74] L.-A. Wu, M. S. Sarandy, and D. A. Lidar, "Quantum phase transitions and bipartite entanglement," *Physical Review Letters*, vol. 93, p. 250404, 2004.

[75] J. Batle and M. Casas, "Nonlocality and entanglement in the XY model," *Physical Review A*, vol. 82, p. 062101, 2010.

[76] J. Maziero, H. C. Guzman, L. C. Céleri, M. S. Sarandy, and R. M. Serra, "Quantum and classical thermal correlations in the XY spin-$\frac{1}{2}$ chain," *Physical Review A*, vol. 82, p. 012106, 2010.

[77] B.-Q. Liu, B. Shao, J.-G. Li, J. Zou, and L.-A. Wu, "Quantum and classical correlations in the one-dimensional XY model with Dzyaloshinskii-Moriya interaction," *Physical Review A*, vol. 83, p. 052112, 2011.

[78] B. Li and Y.-S. Wang, "Quantum correlations in a long range interaction spin chain," *Physica B: Condensed Matter*, vol. 407, no. 1, pp. 77 – 83, 2012.

[79] J. Maziero, L. C. Céleri, R. Serra, and M. Sarandy, "Long-range quantum discord in critical spin systems," *Physics Letters A*, vol. 376, no. 18, pp. 1540 – 1544, 2012.

[80] L. Justino and T. R. de Oliveira, "Bell inequalities and entanglement at quantum phase transitions in the XXZ model," *Physical Review A*, vol. 85, p. 052128, 2012.

[81] W. Cheng, C. Shan, Y. Sheng, L. Gong, S. Zhao, and B. Zheng, "Geometric discord approach to quantum phase transition in the anisotropy XY spin model," *Physica E: Low-dimensional Systems and Nanostructures*, vol. 44, no. 7–8, pp. 1320–1323, 2012.

[82] F. Altintas and R. Eryigit, "Correlation and nonlocality measures as indicators of quantum phase transitions in several critical systems," *Annals of Physics*, vol. 327, no. 12, pp. 3084 – 3101, 2012.

[83] C. C. Rulli and M. S. Sarandy, "Global quantum discord in multipartite systems," *Physical Review A*, vol. 84, p. 042109, 2011.

[84] Y.-C. Li and H.-Q. Lin, "Thermal quantum and classical correlations and entanglement in the XY spin model with three-spin interaction," *Physical Review A*, vol. 83, p. 052323, 2011.

[85] T. Werlang, C. Trippe, G. A. P. Ribeiro, and G. Rigolin, "Quantum correlations in spin chains at finite temperatures and quantum phase transitions," *Physical Review Letters*, vol. 105, p. 095702, 2010.

[86] T. Werlang, G. A. P. Ribeiro, and G. Rigolin, "Spotlighting quantum critical points via quantum correlations at finite temperatures," *Physical Review A*, vol. 83, p. 062334, 2011.

[87] J. Kurmann, H. Thomas, and G. Müller, "Antiferromagnetic long-range order in the anisotropic quantum spin chain," *Physica A: Statistical Mechanics and its Applications*, vol. 112, no. 1–2, pp. 235 – 255, 1982.

[88] T. R. de Oliveira, G. Rigolin, M. C. de Oliveira, and E. Miranda, "Symmetry-breaking effects upon bipartite and multipartite entanglement in the XY model," *Physical Review A*, vol. 77, p. 032325, 2008.

[89] O. F. Syljuåsen, "Entanglement and spontaneous symmetry breaking in quantum spin models," *Physical Review A*, vol. 68, p. 060301, 2003.

[90] A. Osterloh, G. Palacios, and S. Montangero, "Enhancement of pairwise entanglement via Z_2 symmetry breaking," *Physical Review Letters*, vol. 97, p. 257201, 2006.

[91] B. Tomasello, D. Rossini, A. Hamma, and L. Amico, "Ground-state factorization and correlations with broken symmetry," *Europhysics Letters*, vol. 96, no. 2, p. 27002, 2011.

[92] A. Saguia, C. C. Rulli, T. R. de Oliveira, and M. S. Sarandy, "Witnessing nonclassical multipartite states," *Physical Review A*, vol. 84, p. 042123, 2011.

[93] E. Barouch, B. M. McCoy, and M. Dresden, "Statistical mechanics of the XY model I," *Physical Review A*, vol. 2, pp. 1075–1092, 1970.

[94] E. Barouch and B. M. McCoy, “Statistical mechanics of the XY model II. Spin-correlation functions,” *Physical Review A*, vol. 3, pp. 786–804, 1971.

[95] M. S. SARANDY, T. R. D. OLIVEIRA, and L. AMICO, “Quantum discord in the ground state of spin chains,” *International Journal of Modern Physics B*, vol. 27, no. 01n03, p. 1345030, 2013, http://www.worldscientific.com/doi/pdf/10.1142/S0217979213450306.